

Embedded, Doubly-Periodic Minimal Surfaces

Wayne Rossman, Edward C. Thayer*, Meinhard Wohlgemuth†

Abstract

We consider the question of existence of embedded doubly periodic minimal surfaces in \mathbb{R}^3 with Scherk-type ends, surfaces that topologically are Scherk's doubly periodic surface with handles added in various ways. We extend the existence results of H. Karcher and F. Wei to more cases, and we find other cases where existence does not hold.

1 Introduction

H. Karcher [K3] proved the existence of the first complete, embedded, doubly-periodic minimal surface to be found since H. Scherk's classical example, which dates from 1835. We denote Karcher's surface by M_1 (see Figure 1, left). Following this discovery, Wei [We] constructed an embedded, doubly-periodic surface of genus two by adding a handle to M_1 (Figure 1, center). We describe a new embedded, genus two surface that results from adding a different type of handle to M_1 (Figure 1, right), and outline the differences between these two genus two surfaces. In addition, we construct three collections of new, embedded surfaces of genus three that result from adding either two handles of the same type (Figure 2) or two handles of different type (Figure 3).

Using a technique discovered by Karcher-Polthier [KP] to reduce the number of periods to be considered, we are able to add ends to the fundamental piece of each surface presented without increasing the dimension of the period problems, thereby producing countably many different families of new, embedded examples for each of the handle types shown in Figures 1 and 2.

The existence proofs for the genus two surfaces require solving one-dimensional period problems, and the existence proofs for the genus three surfaces require solving either one-dimensional or two-dimensional period problems, depending on the types of handles we choose. When the period problem is one-dimensional (as for surfaces in Figures 1 and 2), we use the intermediate value theorem to solve it. When it is two-dimensional (as for surfaces in Figure 3), we achieve a solution by using a mapping degree argument, a kind of generalization of the intermediate value theorem.

We find that in the two cases of genus three surfaces with four ends and handles of the same type the period problems have no solution. In these exceptional cases we demonstrate a natural geometric obstruction to existence, an obstruction that disappears when more ends are added to the surfaces.

2 Overview of the construction

Karcher's original surfaces M_1 are highly symmetric; they have three mutually perpendicular planes of symmetry and contain four vertical straight lines (see Figures 1, left and 5, left). The three planes divide

*Supported by the National Science Foundation under grants DMS-9011083 and DMS-9312087 and by the U.S. Department of Energy under grant DE-FG02-86ER25015 of the Applied Mathematical Science subprogram of the Office of Energy Research

†Supported by SFB 256 at University of Bonn and the Alexander von Humboldt-Stiftung

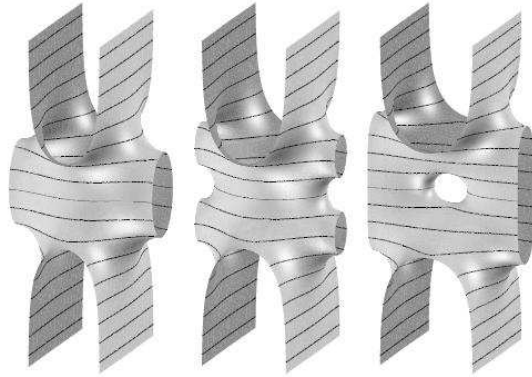


Figure 1: Fundamental pieces of Karcher's surface M_1 (left), Wei's surface M_1^- (center), and M_1^+ (right).

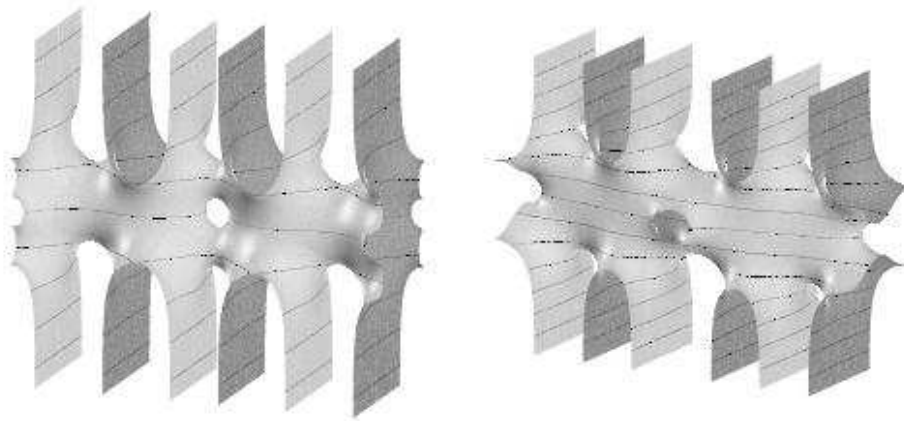


Figure 2: Fundamental pieces of M_3^{--} and M_3^{++}

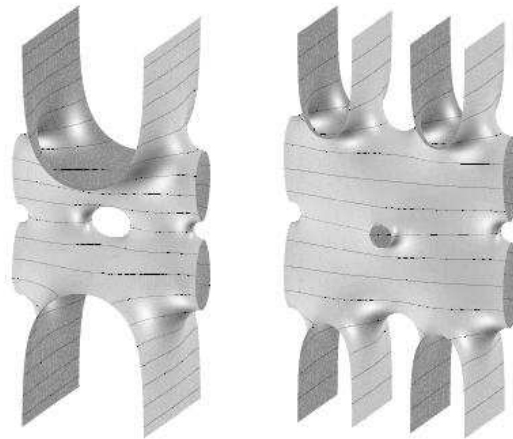


Figure 3: Fundamental pieces of M_1^{+-} (left), and M_2^{+-} (right).

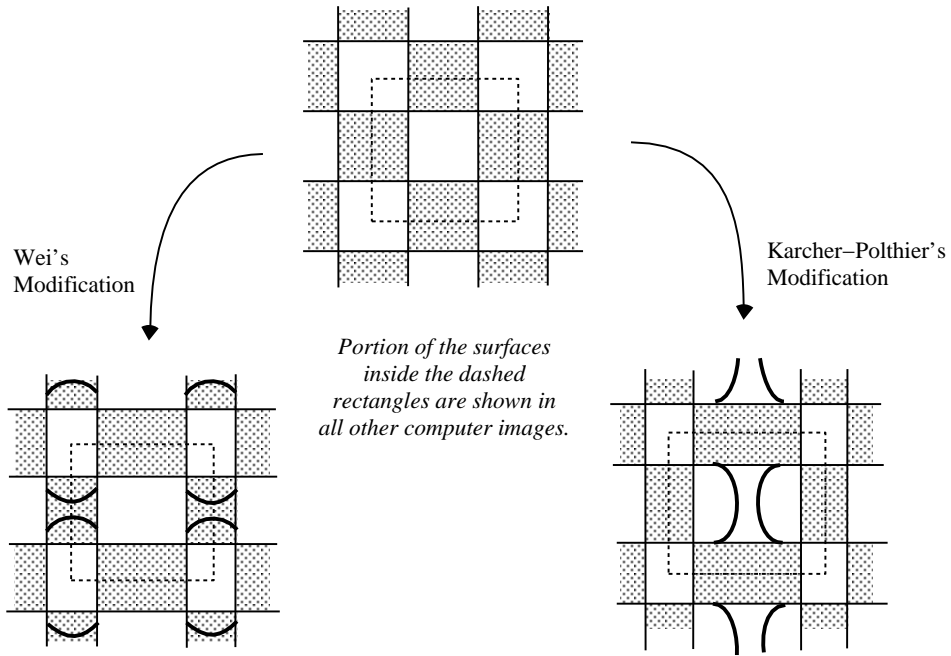


Figure 4: M_1 , M_1^- , and M_1^+ projected onto the x_1 - x_2 plane.

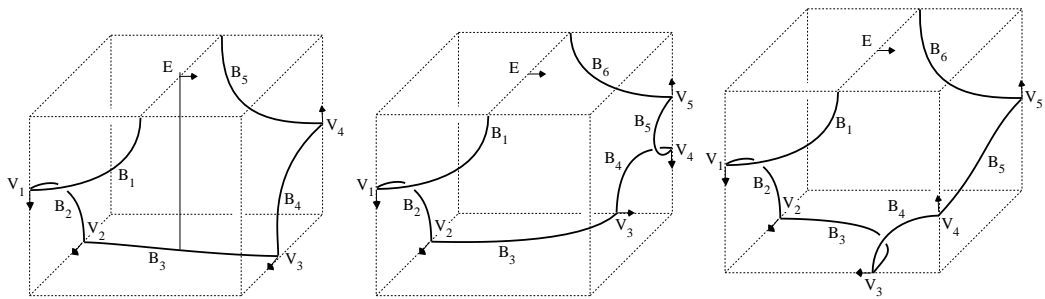


Figure 5: Sketches of one eighth of M_1 (left), M_1^- (center), and M_1^+ (right).

the surface into eight pieces. Each piece is bounded by planar geodesic curves, and has one end. Since all the surfaces we will discuss here share these planar symmetries we will focus on one eighth of these surfaces and draw sketches of this portion only.

The first modification of M_1 was made by F. Wei [We], who constructed a one-parameter family of genus two examples M_1^- by adding a single handle over one of the two saddle points of M_1 (see Figures 1, center and 5, center). Recently it was discovered by Karcher–Polthier [KP] (and the second author independently) that another modification of M_1 was possible. This new surface M_1^+ results from adding a handle to M_1 in a different direction, thereby producing another doubly-periodic, embedded minimal surface of genus two (see Figures 1, right and 5, right).

Remark on notation: *In order to distinguish the two genus two surfaces, we view M_1 from above, imagining that M_1 projects into the black squares of an infinite, black and white checkerboard pattern, with the vertical straight lines projecting onto the corners of these squares (see Figure 4). From this perspective, the handles added by Wei project into the black regions while the new handles project into the white ones. In both cases, the additional handles modify the checker board pattern into a tiling made up of rectangular regions as is indicated in Figure 4. We denote the handles over the black squares with a superscript ‘-’, and those over the white squares with a superscript ‘+’. Hence, in this notation, Wei’s genus two surface is referred to as M_1^- , and the new surface discussed in Section 5 is M_1^+ .*

Each surface discussed in this paper lies in a one-parameter family of embedded surfaces. Since we are interested in the topological qualities of these surfaces, our notation throughout the paper will not reflect the specific surface in the family. The subscript indexes the number of ends on each eighth of the surface.

Both M_1^+ and M_1^- have smaller symmetry groups than Karcher’s original surface; in particular, the vertical straight lines of M_1 are eliminated. The question “Is it possible to add handles to M_1 and preserve the original symmetries?” is a natural one. We might, for example, want to add either a ‘+’ or a ‘-’ type handle and preserve the vertical straight lines. Rotation about these lines (via the Schwarz reflection principle, Theorem 3.1) places another handle over the other saddle point of M_1 . This would result in a genus three surface with four Scherk ends. It is easy to imagine such a surface for either type of handle. Indeed, the suggested conjugate contour of one eighth of either surface supports a Plateau solution that is a Jenkins-Serrin graph [JS]. So a minimal surface with boundary exists with the desired shape, but we only know that certain bounding planar curves lie in parallel planes. We then must solve the one-dimensional period problem or, equivalently, show that the parallel planes coincide. We will prove that neither of these period problems are solvable, and we do so by finding natural obstructions on the corresponding conjugate surfaces. Understanding these obstructions, we realize it is possible to overcome them by adding more ends to each surface. Because of the desired symmetries, each eighth of these surfaces must have an odd number of ends. Indexing by this number, we show the period problems are never solved on M_1^{--} and M_1^{++} , and that for $k \geq 1$ the period problems associated to M_{2k+1}^{--} and M_{2k+1}^{++} are solvable. The superscript indicates the types of handles added to M_1 . See Figure 2.

With the addition of each new end, there is a new associated period. In Section 4, we describe a technique found by Karcher–Polthier [KP] that shows that one may simultaneously solve these end periods. Specifically, they observed that a certain simple restriction on the conjugate contours ensures these end periods are all zero. Moreover, this restriction leaves an ample number of parameters free to allow us to adjust the other periods associated with the new handles.

Instead of adding two handles of the same type to M_1 , we may also consider surfaces which have two

handles of different types. This produces a family of genus three surfaces that no longer have the straight line symmetries of M_1 . Without this additional symmetry, the period problem resulting from the new handles is two-dimensional. The third author's experience with two-dimensional period problems [Wo] suggested that these period problems may be solvable. We prove in Section 9 that M_1^{+-} with four Scherk-type ends exists. Generalizing the examples M_1^{+-} to have $4k$ Scherk-type ends for $k \geq 2$, numerical evidence suggests the existence of M_k^{+-} for $k \geq 2$ (see Figure 3).

The computer graphics in the figures were created using the MESH software produced by James T. Hoffman of the Mathematical Sciences Research Institute, Berkeley, California, U.S.A..

3 Background results needed for the construction

We consider only connected and properly immersed minimal surfaces. To establish notation we state the following description of the Weierstrass Representation.

Weierstrass-Representation: Let M be a minimal surface in \mathbb{R}^3 and R the underlying Riemann surface of M . Then M can be expressed, up to translations, in terms of a meromorphic function g on R , the so-called Gauss map (since g will be stereographic projection of the oriented normal vector of M), and a holomorphic differential η on R by

$$F(p) = Re \int_{p_0}^p (\phi_1, \phi_2, \phi_3) \quad , \quad (3.1)$$

where $p_0 \in R$ is fixed and

$$(\phi_1, \phi_2, \phi_3) = \left(\left(\frac{1}{g} - g \right) \eta, i \left(\frac{1}{g} + g \right) \eta, 2\eta \right) . \quad (3.2)$$

Conversely, let R be a Riemann surface, g a meromorphic function on R , and η a holomorphic differential on R . Then (3.1) and (3.2) define a conformal minimal immersion $F : R \rightarrow \mathbb{R}^3$, provided the poles and zeros of order ℓ of g coincide with the zeros of order ℓ of η , and (ϕ_1, ϕ_2, ϕ_3) has no real periods, i.e.

$$\text{Period}_{(\phi_1, \phi_2, \phi_3)}(\gamma) = \int_{\gamma} (\phi_1, \phi_2, \phi_3) \in i\mathbb{R} \quad (3.3)$$

for all closed curves γ on R .

We call (R, g, η) the *Weierstrass data* of the minimal surface M . Denoting the universal cover of R by \tilde{R} , the minimal immersion $F^* : \tilde{R} \rightarrow \mathbb{R}^3$ with the Weierstrass data $(R, g, i\eta)$ is called the *conjugate surface* to M , and is denoted by M^* . It is known that any curve of R which is mapped by F to a non-straight planar geodesic of M is mapped by F^* to a straight line in M^* . Furthermore, since the Gauss map g and the first fundamental form are the same for both M and M^* , it follows that the planar geodesic in M will lie in a plane perpendicular to the corresponding line in M^* and that the planar geodesic in M will have the same length as the line in M^* . We will use these properties extensively. The following known results are also central to the arguments we will be making.

Theorem 3.1 (Schwarz reflection principle) *If a minimal surface $M \subset \mathbb{R}^3$ with boundary contains a non-straight planar geodesic \mathcal{C} (resp. straight line \mathcal{C}) in its boundary, then M can be extended smoothly across \mathcal{C} by reflecting through the plane containing \mathcal{C} (resp. rotating about \mathcal{C}).*

Theorem 3.2 (Krust [DHKW]) *If an embedded minimal surface $F : B \rightarrow \mathbb{R}^3$, $B = \{w \in \mathbb{C} : |w| < 1\}$ can be written as a graph over a convex domain in a plane, then the conjugate surface $F^* : B \rightarrow \mathbb{R}^3$ is also a graph over a domain in the same plane.*

Theorem 3.3 (Jenkins-Serrin [JS]) *Let D be a bounded convex domain such that ∂D contains two sets of finite numbers of open straight segments $\{A_i\}, \{B_j\}$ with the property that no two segments A_i and no two segments B_j have a common endpoint. Let the remaining portion of ∂D consist of a finite number of open arcs $\{C_k\}$, and of endpoints of A_i, B_j , and C_k . Let \mathcal{P} denote a simple closed polygon whose vertices are chosen from among the endpoints of the A_i and B_j . Let*

$$\alpha = \sum_{A_i \subset \mathcal{P}} \text{length}(A_i), \quad \beta = \sum_{B_j \subset \mathcal{P}} \text{length}(B_j), \quad \gamma = \text{length of perimeter of } \mathcal{P}.$$

Then if $\{C_k\} \neq \emptyset$, there exists a solution of the minimal surface equation in D which assumes the value $+\infty$ on each A_i , $-\infty$ on each B_j , and any assigned bounded continuous data on each open arc C_k if and only if

$$2\alpha < \gamma \text{ and } 2\beta < \gamma$$

for each polygon \mathcal{P} chosen as above. Moreover, the solution is unique when it exists.

Remark 3.1 *Note that in Theorem 3.3, we allow the possibility that two different C_k have a common endpoint. We may have jump discontinuities in the boundary data at the points where two different C_k meet. It follows from the arguments in [JS] that, for D as in Theorem 3.3, if u_1 and u_2 are two solutions of the minimal surface equation such that $u_1 = u_2 = +\infty$ on each A_i and $u_1 = u_2 = -\infty$ on each B_j and $u_1 \geq u_2$ on each C_k , then $u_1 \geq u_2$ in the interior of D .*

4 The Examples M_k

An immediate application of Theorems 3.2 and 3.3 is to prove that one can add more ends to Karcher's genus one surface M_1 , thereby creating the surfaces M_k .

Theorem 4.1 *For each $k \geq 2$, there exists a one-parameter family M_k of embedded, doubly-periodic minimal surfaces of genus one with $4k$ Scherk-type ends.*

Proof. Fix k . The conjugate boundary of one eighth of M_k is a graph over a rectangular domain with three sides at height zero and the fourth edge subdivided into k segments with heights alternating between $+\infty$ and $-\infty$. Theorem 3.3 yields a Plateau solution with this boundary. Then Theorem 3.2, together with Theorem 3.1 and the maximum principle, gives the embedded surfaces M_k from these solutions. The period problems associated to the ends, which equal the residues at the end punctures on the compact Riemann surface, are solved by choosing the A_i and B_j to all be of the same length. Varying the length of the opposing zero height sides of the rectangular domain yields a one-parameter family of surfaces.

On the other hand, we immediately have:

Corollary 4.1 *M_k is a k -fold covering of M_1 .*

Proof. Schwarz reflection (Theorem 3.1) about line segments on the bounding conjugate contour for M_1 produces the bounding conjugate contour for M_k for any k . The uniqueness of the minimal graphs in Theorem 3.3 completes the proof.

We included these examples M_k because the technique used to solve the k -dimensional period problem arising from the additional ends is used throughout the paper. In particular, we have

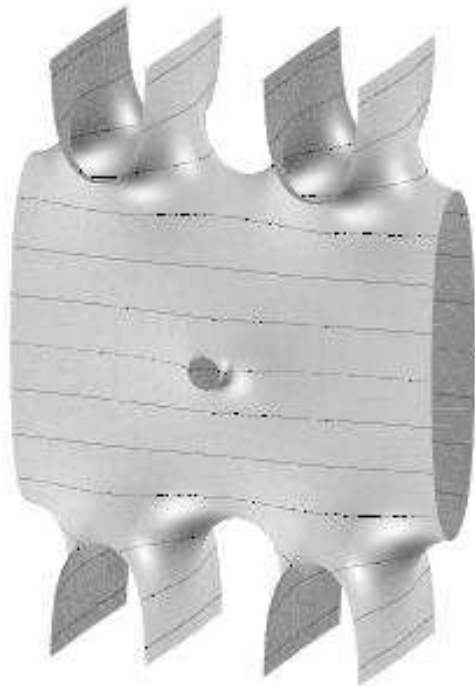


Figure 6: Fundamental piece of M_2^+ .

Lemma 4.1 *Each collection of surfaces, M_k^+ , M_k^- , M_{2k+1}^{++} , M_{2k+1}^{--} , M_k^{+-} , results from adding ends and handles to M_1 , and the period problems arising from the additional ends are all solved as above, i.e. by requiring*

$$\epsilon = \text{length}(A_i) = \text{length}(B_j)$$

to be constant for all i, j .

A proof of this lemma is contained in the appendix of this paper.

The observation that this restriction on the conjugate contour solves all the periods arising from additional ends demonstrates that these periods are independent of the periods arising from additional handles. This restriction enables us to eliminate all but one or two periods in these surfaces, so we may focus only on the periods arising from the new handles.

5 The Examples M_k^+

The sketch in Figure 7, upper-left is of a contour suggestive of a ‘+’ type handle in an even ended surface which we will use to motivate the discussion. Taking its conjugate contour produces the contour in Figure 7, upper-right, which is bounded by line segments as labelled in the figure. This contour bounds a Jenkins-Serrin graph over the front face of the box and hence supports a solution to the Plateau problem. Let $\beta_j = \text{Length}(B_j) = \text{Length}(B_j^*)$ for $j = 2, 3, 4, 5$. The symmetries of M_k^+ imply there are k periods, $k - 1$ of these resulting from the ends, and one arising from the new handle. Lemma 4.1 implies that if we restrict the conjugate contours so that the lengths of the segments over which the boundary contour is unbounded are equal, then $k - 1$ of these periods are zero. Let $\epsilon = \beta_3/k$ be this common length.

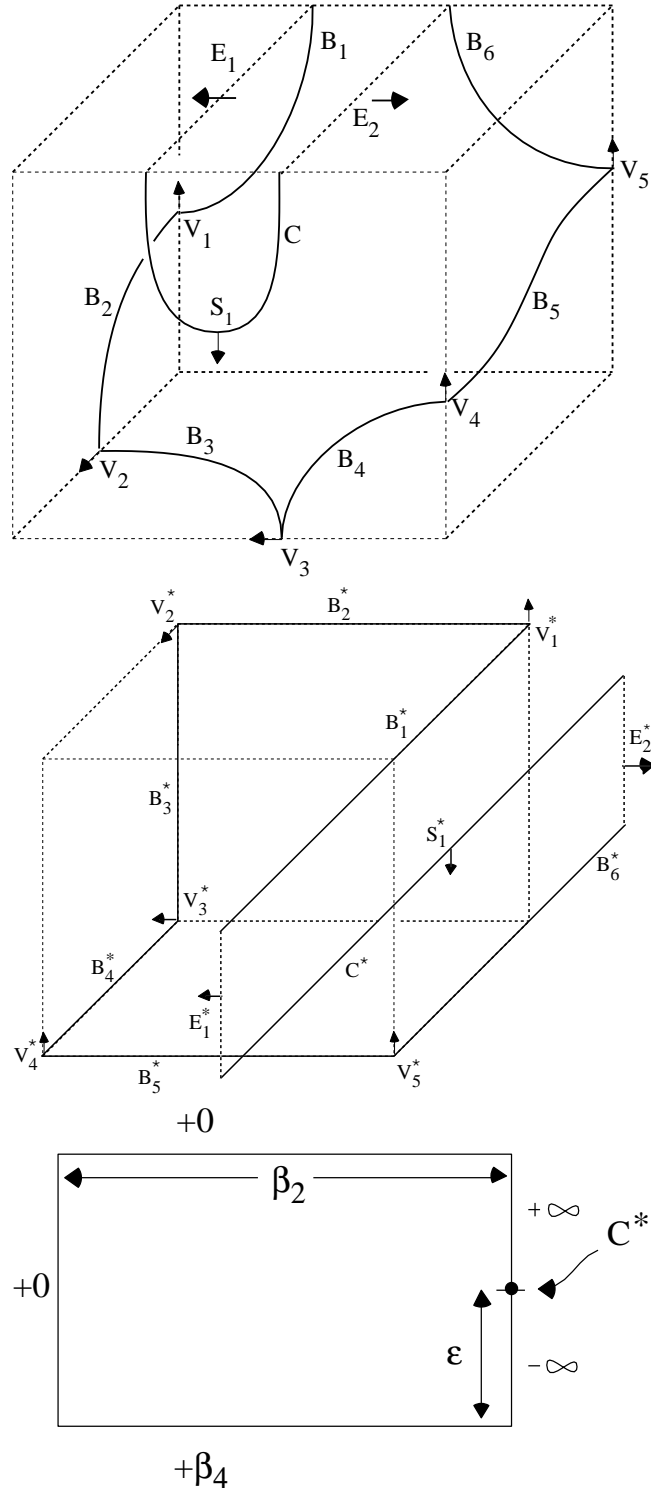


Figure 7: Sketches of the boundaries of one eighth of M_2^+ and its conjugate (top row), and the graph dimensions and heights over the front face of the bounding box for the conjugate contour (bottom).

The remaining period is shown to change sign as β_4 is varied so that the intermediate value theorem implies the following

Theorem 5.1 *For each $k > 0$, there exists a one-parameter family M_k^+ of embedded, doubly-periodic minimal surfaces of genus two with $4k$ Scherk type ends.*

We give the argument only for the case $k = 2$, as the argument is essentially identical for all k . Choosing the curves B_2^* and B_3^* to lie at the zero level, the height of B_5^* is $+\beta_4$, with the end E_1^* at height $+\infty$ and E_2^* at $-\infty$ as indicated in Figure 7, bottom.

Proof. All that remains to be shown is that as β_4 is varied, the period $\pi(\beta_4) = \operatorname{Re} \int_{S_1}^{V_4} \phi_2$ changes signs. Note that this period measures the distance between the planes containing the curves B_4 and C .

Let $\beta_2 > \epsilon$ and consider the two cases of β_4 large and β_4 small:

a) Let $\beta_4 \rightarrow 0$. The limiting surface is M_2 and the embeddedness of M_2 implies the point V_4 lies behind the symmetry plane of C ; so $\pi(\beta_4) < 0$ for β_4 near zero.

b) For large β_4 , we claim the distance between the planes containing B_4 and B_6 is $\beta_2 - \delta > \epsilon$, since the Gauss map approaches a constant along B_5 . To see this, use the barrier surface given as a Jenkins-Serrin graph over the back face of the box in Figure 7, right, with height $+\infty$ over the edge B_5^* and the same heights as the contour for M_2^+ over all other edges. Arguments in [JS] imply the conjugate graphs converge to the barrier surface as $\beta_4 \rightarrow \infty$. So in the limit, the behavior of the ends is the same and therefore B_5 approaches a straight line of length β_2 which is greater than ϵ . Hence B_4 lies in front of C and $\pi(\beta_4) > 0$ for β_4 large.

Hence the period problem is solvable. Since β_2 is only bounded below this shows the period problem can be solved for each $\beta_2 > \epsilon$ and therefore there exists a one-parameter family of these surfaces. Theorem 3.2 implies each eighth of any one of these surfaces is embedded and, by Theorem 3.1, extends to an embedded minimal surface.

Weierstrass data for M_k^+ : Since M_k^+ is invariant under an order-two normal symmetry about the x_3 -axis, with six fixed points, the quotient is a sphere minus $2k$ points. The meromorphic function g^2 , where g is the Gauss map, descends to the quotient. Taking z to be the coordinate on this sphere, we normalize so that $z(V_3) = 0$, $z(V_2) = \infty$ and $e_k = z(E_k) = 1$. Define v_i by $v_i = z(V_i)$ for $i = 1, 4, 5$, $s_j = z(S_j)$, $j = 1, 2, \dots, k-1$, where $\{S_j\}$ are the vertical points lying on the planar geodesics between the ends, $e_m = z(E_m)$, $m = 1, \dots, k-1$. Conformality of z orders these values $0 < v_4 < v_5 < 1 < s_{k-1} < e_{k-1} < s_{k-2} < \dots < s_1 < e_1 < v_1$.

Comparison of the meromorphic functions g^2 and z leads to the following Weierstrass data for M_k^+ :

$$\begin{aligned}
 g^2 &= \frac{z + v_4}{z - v_4} \frac{z + v_5}{z - v_5} \frac{z + (-1)^k v_1}{z - (-1)^k v_1} \cdot f_k^2(z, s_1, \dots, s_{k-1}), \\
 \eta &= \frac{dz}{\mathcal{E}_k(z, e_1, \dots, e_k)} D_k(z, s_1, \dots, s_{k-1}) N_k(z, s_1, \dots, s_{k-1}),
 \end{aligned} \tag{5.1}$$

where $f_k(z, s_1, \dots, s_{k-1}) = N_k(z, s_1, \dots, s_{k-1})/D_k(z, s_1, \dots, s_{k-1})$, with

$$\begin{aligned} N_k(z, s_1, \dots, s_{k-1}) &:= \prod_{j=1}^{k-1} (z + (-1)^{k+j} s_j), \\ D_k(z, s_1, \dots, s_{k-1}) &:= \prod_{j=1}^{k-1} (z - (-1)^{k+j} s_j), \\ \mathcal{E}_k(z, e_1, \dots, e_k) &:= \prod_{m=1}^k (z^2 - e_m^2). \end{aligned}$$

The conditions for embedded ends are

$$g^2(1) = g^2(e_m) = 1 \quad (5.2)$$

for all $m \leq k$. For $k = 2$, we have the constraints

$$\begin{aligned} A(1 + v_4)(1 + v_5) &= \tilde{A}(1 - v_4)(1 - v_5) \\ B(e_2 + v_4)(e_2 + v_5) &= \tilde{B}(e_2 - v_4)(e_2 - v_5), \end{aligned}$$

where $A = (1 - s_1)^2(1 + v_1)$, $\tilde{A} = (1 + s_1)^2(1 - v_1)$, $B = (e_1 - s_1)^2(e_1 + v_1)$, and $\tilde{B} = (e_1 + s_1)^2(e_1 - v_1)$. From this, we can derive the conditions

$$v_4 v_5 = \frac{(A - \tilde{A})(B + \tilde{B})e_1 - (A + \tilde{A})(B - \tilde{B})e_1^2}{(A + \tilde{A})(B - \tilde{B}) - (A - \tilde{A})(B + \tilde{B})e_1}, \quad (5.3)$$

$$v_4 + v_5 = \frac{(A - \tilde{A})(B + \tilde{B})(e_1^2 - 1)}{(A + \tilde{A})(B - \tilde{B}) - (A - \tilde{A})(B + \tilde{B})e_1}. \quad (5.4)$$

And v_4 and v_5 are the zeros of a degree-two polynomial.

With the Weierstrass data (5.1) and the constraints (5.3) and (5.4) we get the image in Figure 6 after choosing $k = 2$ and determining the correct values for v_1 and e_1 .

6 The Examples M_k^-

The periods associated to M_k^- arise as residues at the punctures for the ends or from integrating along a curve representing a non-trivial homotopy class. As in the case of M_k , the residues at the ends are made equal by equally distributing the straight lines lying between the ends of the conjugate of one-eighth of the fundamental piece. The portion of the period problem resulting from non-trivial homotopy classes is one-dimensional due to the symmetries of M_k^- , and use of the same barriers as in [We] shows that this period is also solvable. Hence

Theorem 6.1 *There exists a one-parameter family of genus two, embedded minimal surfaces M_k^- with $4k$ Scherk-type ends, for all $k \geq 1$.*

7 The Examples M_{2k+1}^{--}

In this section, we construct the embedded minimal surfaces M_{2k+1}^{--} . Specifically, we construct genus three surfaces having all the symmetries of Karcher's genus one surface M_1 , with two '–' handles and $4(2k + 1)$ Scherk ends.

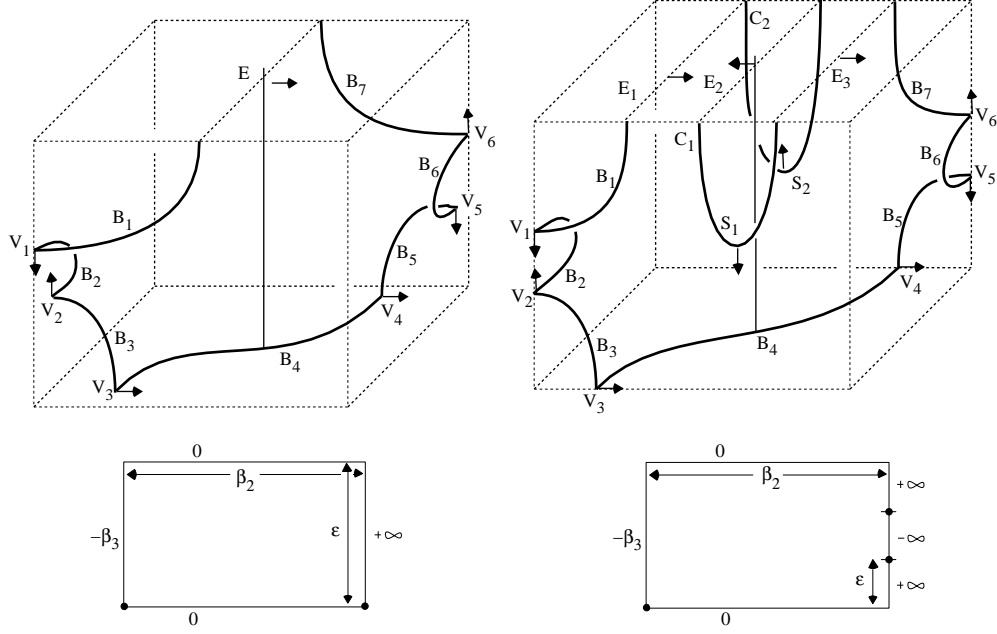


Figure 8: Sketches of the boundary of one eighth of M_1^{--} (upper left) and M_3^{--} (upper right) with the parameters for the conjugate boundary contour viewed as a graph over the rectangular region drawn below each sketch.

F. Wei modified M_1 by introducing a single handle over one of its saddle points. In the sketches of Figure 5, one can see that this results in a new vertical point over V_4 . In order to retain the vertical straight lines of M_1 on higher genus surfaces, one is obliged to add a handle over the other saddle point, since, by Theorem 3.1, 180° rotation about these straight lines are isometries of the surface. Such a surface might have a boundary like that sketched in Figure 8, left. If this surface did exist, its conjugate contour would be as in Figure 8, lower left. This conjugate contour meets all the conditions of Theorem 3.3, hence it supports a solution to the Plateau Problem, and the original surface conjugate to this solution is a minimal surface bounded by planar curves with the desired symmetries.

Although the conjugate surface is a minimal surface bounded by planar curves, it is not guaranteed that reflection in these planes produces an embedded doubly-periodic surface. In particular, using the notation of Figure 8, one does not know if the curves B_1 and B_3 lie in the same plane. This brings us to the period problem; one must insure that the planes containing B_1 and B_3 coincide. Since we have assumed the surface contains a vertical straight line, knowing B_1 and B_3 lie in the same plane implies the planes containing B_5 and B_7 also coincide. Should this period problem be solvable, the surface in our notation would be denoted by M_1^{--} .

In Theorem 7.1.2 we prove, by analyzing the Plateau solutions for the countour of Figure 8, lower left, that this period problem can never be solved. In contrast, by having more ends on the surface, as in Figure 8, right, we prove in Theorem 7.1.1 that the obstruction to solving this period problem is removed. These new surfaces are the surfaces M_{2k+1}^{--} in our notation.

Theorem 7.1 (1) *For each $k \geq 1$, there exists a one-parameter family of embedded, doubly-periodic minimal surfaces M_{2k+1}^{--} of genus three;*

(2) M_1^{--} does **not** exist.

Proof. Let $\beta_j = \text{Length}(B_j) = \text{Length}(B_j^*)$ for $j = 2, 3, 4, 5, 6$. By Lemma 4.1, all periods arising from the addition of ends are zero provided the lengths of the segments over which the conjugate contours are unbounded are equal. We assume this condition, and let ϵ be this common length, which remains fixed throughout the proof. Hence we need only address the periods arising from non-trivial homotopy classes, i.e. from the addition of new handles. Note that from the conjugate contour one sees that for each M_{2k+1}^{--} , $\beta_4 = (2k + 1)\epsilon$.

Proof of (2): We proceed by contradiction. Suppose M_1^{--} does exist. Let S be one eighth of M_1^{--} . Figure 8, left shows a sketch of S . We are assuming that there is a vertical straight line on S passing through the end E , orthogonal to the plane containing B_4 . Rotation about this line interchanges V_1 and V_6 , and interchanges V_2 and V_5 .

Remark 7.1 *The boundary contour of S^* is a graph over a rectangle as drawn in Figure 8, lower left, and as a result of the symmetries, B_2^* and B_6^* lie at the same height. Choosing this to be the zero height implies the line B_4^* has height $-\infty < -\beta_3 < 0$, and the end E has height $+\infty$. From Theorem 3.3, we get a minimal graph with this boundary. As a graph, it is embedded and Theorem 3.2 assures that S is embedded. Hence there exists a Plateau solution S^* with the desired boundary and symmetries.*

Claim: *The distance between the planes containing B_3 and B_5 is always shorter than the distance between the planes containing B_1 and B_7 . Hence the period is always of the same sign.*

The planar geodesic B_4 has length ϵ and is not a straight line. Therefore the distance between the symmetry planes containing B_3 and B_5 is strictly less than $\beta_4 = \epsilon$, and the curve B_3 always lies to one side of the plane containing B_1 . This establishes the claim and completes the proof of (2).

In summary, the period problem on M_1^{--} is unsolvable because the distance ϵ between the planar curves bounding the end is equal to β_4 and the planar curve B_4 is not straight. If one could modify the conjugate contour so that $\beta_4 > \epsilon$, then the period problem may be solvable. One way of achieving this is to add more ends to the conjugate contour as in the sketch in Figure 8, lower right. Because we wish to maintain the vertical straight lines, the contour bounded by straight lines must have a horizontal planar symmetry. Therefore we must add an even number of extra ends. Figure 8, right is a sketch of such a surface with three ends. The conjugate contour for this surface is again a Jenkins-Serrin graph over a rectangle as drawn in Figure 8, lower right.

Proof of 1): Assume $\beta_2 > \beta_4 = (2k + 1)\epsilon$. Since we have assumed the existence of a vertical straight line on the surface passing thru E_{k+1} and orthogonal to B_4 , we have only one period arising from a non-trivial homotopy class. For this period, we must show that B_1 lies in the plane containing B_3 . We use the intermediate value theorem to show the existence of a value for β_3 such that this period is zero. Specifically we have two cases:

a) As $\beta_3 \rightarrow 0$, M_{2k+1}^{--} degenerates to M_{2k+1} . By the embeddedness of M_{2k+1} , we have the point V_2 moves behind the plane containing B_1 , and the period is negative.

b) As $\beta_3 \rightarrow \infty$, the curve B_4^* moves away toward height $-\infty$. Let \mathcal{B} be the Jenkins-Serrin graph over the rectangle as described in Figure 8, lower right, with boundary heights $0, -\infty, 0, +\infty, -\infty, +\infty$ with zero heights corresponding to the edges containing the curves B_2^* and B_6^* . This graph \mathcal{B} exists, since $\beta_2 > \beta_4$, by Theorem 3.3. By the arguments in [JS], the conjugate graphs converge to \mathcal{B} as $\beta_3 \rightarrow \infty$. Therefore along B_4^* the Gauss map approaches a constant value, and the displacement along B_4 in the desired direction

approaches $(2k+1)\epsilon = \beta_4$. Hence V_2 lies in front of the plane containing B_1 for large β_3 , and the period is positive.

By the intermediate value theorem, there exists a value of β_3 at which the period is zero. Therefore the period problem is solvable on M_{2k+1}^{--} .

Theorems 3.3 and 3.2 imply that the one eighth portion S of M_{2k+1}^{--} is embedded. Applying the classical maximum principle and the maximum principle at infinity [MR], one easily determines that the full fundamental piece of M_{2k+1}^{--} lies inside the box given by its boundary curves. Reflections through the faces of this box produces an embedded surface. Therefore M_{2k+1}^{--} is embedded.

β_2 has not been used in this argument (β_2 is any fixed number greater than β_4), and therefore we have a one-parameter family of M_{2k+1}^{--} for each $k \geq 1$.

Weierstrass data for M_3^{--} : Since M_3^{--} is invariant under an order-two normal symmetry about the x_3 -axis, with eight fixed points, the quotient surface is a sphere. The meromorphic function g^2 , where g is the stereographic projection of the Gauss map, descends to the quotient. Taking z to be the coordinate on the sphere, we normalize so that $z(V_3) = \infty$, $z(V_4) = 0$, and $z(E_2) = 1$. With this normalization, rotation about the vertical straight line on M_3^{--} corresponds to inversion through the unit circle. Define $e_1 = z(E_1)$, $v_j = z(V_j)$, for $j = 1, 2$, and $s_1 = z(S_1)$. Then $z(E_3) = 1/e_1$, $z(V_5) = 1/v_2$, $z(V_6) = 1/v_1$, and $z(S_2) = 1/s_1$. Comparison of the meromorphic functions g^2 and z leads to the following Weierstrass data for M_3^{--} :

$$\begin{aligned} g^2 &= \frac{z-v_1}{z+v_1} \frac{z+1/v_1}{z-1/v_1} \frac{z+v_2}{z-v_2} \frac{z-1/v_2}{z+1/v_2} \left(\frac{z-s_1}{z+s_1} \right)^2 \left(\frac{z+1/s_1}{z-1/s_1} \right)^2, \\ \eta &= \frac{dz}{z^2-1} \frac{z^2-s_1^2}{z^2-e_1^2} \frac{z^2-1/s_1^2}{z^2-1/e_1^2}. \end{aligned} \tag{7.1}$$

This Weierstrass data insures each Scherk-type end is itself an embedded end, but one must also guarantee that the limit normals on the ends are antipodal so the ends do not cross each other as they diverge. Because of our choice of orientation, this is equivalent to the conditions

$$g^2(1) = g^2(e_1) = g^2(1/e_1) = 1.$$

Due to the rotational symmetry, the second and third conditions result in the same constraints, while the first is automatically satisfied. The second condition places the following constraint on e_1 :

$$\begin{aligned} (\delta + \gamma + 2\nu)e_1^6 &+ [(\delta + \gamma)(\nu^2 - 1) + 2(\delta\gamma - 2)\nu - (\delta + \gamma) - 2\nu] e_1^4 \\ &+ [2\nu - (\delta + \gamma)(\nu^2 - 2) - 2\nu(\delta\gamma - 2) + (\delta + \gamma)] e_1^2 \\ &- 2\nu - (\delta + \gamma) = 0, \end{aligned} \tag{7.2}$$

where $\delta = v_2 - 1/v_2$, $\gamma = 1/v_1 - v_1$, and $\nu = 1/s_1 - s_1$.

By Theorem 7.1, there exists a solution to (7.2) in the necessary range. Using the computer to find this solution and to calculate the values of the two periods of the Weierstrass data, we determine the appropriate values for e_1 , v_1 , and v_2 , given a value for s_1 . We thereby generate the image of M_3^{--} in Figure 2.

8 The Examples M_{2k+1}^{++}

As in the previous section, one might investigate whether it is possible to construct genus three examples by adding two '+' type handles to M_1 while preserving the symmetries. The same methods as those used in

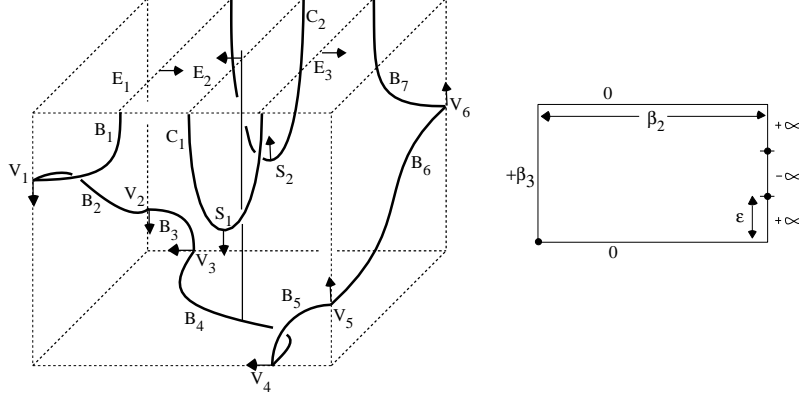


Figure 9: Sketches of the boundary of one eighth of M_3^{++} and its conjugate boundary graph heights over the front face of the bounding box.

the ‘-’ case can be used to show the existence of a minimal disc with the desired boundary and symmetries, but one must again consider the period problem. The similarities between the conjugate contours for the two ‘-’ handles and two ‘+’ handles allow one to observe a similar natural obstruction to solving the period problem for the one-ended surfaces. By adding more ends to these surfaces, as in the previous section, this obstruction is overcome. Denoting these new surfaces by M_{2k+1}^{++} and using arguments similar to those used in the proof of Theorem 7.1, one has:

- Theorem 8.1** 1) *There exists a one-parameter family of embedded, doubly-periodic minimal surfaces M_{2k+1}^{++} of genus three, for each $k \geq 1$.*
 2) M_1^{++} *does not exist.*

Note: The symmetry groups for M_1 , M_{2k+1}^{--} , and M_{2k+1}^{++} are identical. Hence one has two collections of genus three minimal surfaces with the same symmetries as Karcher’s original genus one surface M_1 .

Weierstrass data for M_3^{++} : Using the same notation as that used for the surface M_3^{--} , we can determine the Weierstrass data for M_3^{++} ; the results are as follows:

$$g^2 = \frac{z - v_1}{z + v_1} \frac{z + 1/v_1}{z - 1/v_1} \frac{z - v_2}{z + v_2} \frac{z + 1/v_2}{z - 1/v_2} \left(\frac{z - s_1}{z + s_1} \right)^2 \left(\frac{z + 1/s_1}{z - 1/s_1} \right)^2,$$

$$\eta = \frac{dz}{z^2 - 1} \frac{z^2 - s_1^2}{z^2 - e_1^2} \frac{z^2 - 1/s_1^2}{z^2 - 1/e_1^2}.$$

With the same constraints for parallel ends as in (7.2) and by changing γ to $v_1 - 1/v_1$ we compute the parameters used in generating the image in Figure 2.

9 The Examples M_k^{+-}

In this section, we consider the genus three surfaces M_k^{+-} which arise by adding both a ‘+’ handle and a ‘-’ handle to M_k . As in the case of M_k^- and M_k^+ , the handles make it impossible to preserve the straight line symmetries of M_1 , but the three mutually perpendicular planar reflectional symmetries are preserved. These symmetries reduce the number of periods that need to be addressed in order for the period problem to be

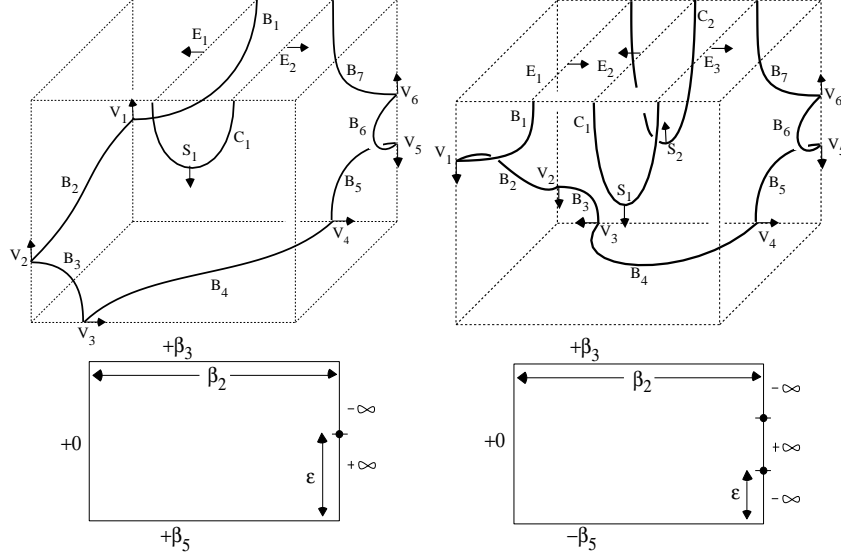


Figure 10: Sketches of one eighth of M_2^{+-} (upper left) and M_3^{+-} (upper right) with the Jenkin–Serrin graph boundary heights for the conjugates of each eighth drawn below.

solved. In particular, M_k^{+-} has $k+1$ periods: $k-1$ of these periods arise from the residues of the Weierstrass data at the ends; leaving only two periods resulting from non-trivial homotopy classes. By Lemma 4.1, the periods resulting from the additional ends are simultaneously zero provided the segments over which the conjugate contours are unbounded are equal in length. As we have done in the previous sections, we fix ϵ to be this common length. Now we need only consider the two periods that result from non-trivial homotopy classes.

Figure 10 contains sketches of the boundary of one eighth of M_2^{+-} (left) and M_3^{+-} (right), together with the conjugate contour heights written as a graph, where $\beta_j = \text{Length}(B_j)$ for $j = 2, 3, 4, 5, 6$. We assume $\beta_2 > \epsilon$ on all contours.

We now consider the case $k = 1$. By consideration of the two periods for M_1^{+-} for varying values of β_3 and β_5 , we are able to use a two-dimensional degree argument to prove:

Theorem 9.1 *There exists a one-parameter family of genus three, embedded minimal surfaces M_1^{+-} with 4 Scherk-type ends.*

In particular, we consider the periods along the curves in the (β_3, β_5) plane given by

$$\begin{aligned} \tau_1 &= (0, \beta_5) \text{ for } \beta_5 \in [0, T], & \tau_2 &= (\beta_3, T) \text{ for } \beta_3 \in [0, S], \\ \tau_3 &= (S, \beta_5) \text{ for } \beta_5 \in [0, T], & \tau_4 &= (\beta_3, 0) \text{ for } \beta_3 \in [0, S], \end{aligned}$$

for positive S and T , and are able to show that, with the correct choices for β_2 , S , and T , these curves surround a solution for the period problem.

The conjugate contours for M_1^{+-} associated to points along the curves τ_1 and τ_4 degenerate to conjugate contours for either known surfaces or surfaces which are known to have unsolvable period problems. When the degenerate contour is known to have a solvable period problem, we assume nothing about the values of these periods, and in general the remaining unfixed parameter which we will not specify has been shown to

control this period. We seek to use only the general shape of the degenerate contours and not the solvability of the period problems on the lower genus minimal surfaces. On each of the degenerate surfaces, the labels we use are inherited from the contour for M_1^{+-} , which may differ from those used previously in the text.

Proof of Theorem 9.1. Consider one-eighth of the fundamental piece, analogous to the depictions of M_2^{+-} and M_3^{+-} in Figure 10. This one-eighth piece is bounded by seven planar geodesics B_1, \dots, B_7 . B_1 and B_7 are each of infinite length with a single endpoint, and B_2, \dots, B_6 are each finite length curve segments. Let $\beta_j = \text{Length}(B_j)$ for each $j = 2, 3, 4, 5, 6$. The singular points of the boundary are $V_j = B_j \cap B_{j+1}$ for $j = 1, \dots, 6$. (Unlike the cases when $k \geq 2$, there are no curves C_j , as in Figure 10.) We place the surface so that g equals 1 at the single end E_1 and equals 0 at V_1 , and we define the functions

$$\begin{aligned}\pi_1(\beta_2, \beta_3, \beta_5) &= \operatorname{Re} \int_{V_3}^{V_4} \phi_2 = \operatorname{Re} \int_{V_2}^{V_4} \phi_2, \\ \pi_2(\beta_2, \beta_3, \beta_5) &= \operatorname{Re} \int_{V_4}^{V_6} \phi_2 = \operatorname{Re} \int_{V_5}^{V_6} \phi_2,\end{aligned}$$

where ϕ_2 is the second component of the Weierstrass map given in equation (3.2). We will show that:

- i)* $\pi_1(\tau_j)$ and $\pi_2(\tau_j)$ change monotonically on each τ_j , for $j = 1, 2, 3, 4$. In particular, for each fixed β_2 and β_5 , $\pi_1(\beta_2, \beta_3, \beta_5)$ is a strictly decreasing function of β_3 ; for each fixed β_2 and β_3 , $\pi_1(\beta_2, \beta_3, \beta_5)$ is a strictly increasing function of β_5 ; for each fixed β_2 and β_5 , $\pi_2(\beta_2, \beta_3, \beta_5)$ is a strictly decreasing function of β_3 ; and for each fixed β_2 and β_3 , $\pi_2(\beta_2, \beta_3, \beta_5)$ is a strictly decreasing function of β_5 .
- ii)* For all $\beta_2 > \epsilon$, $\pi_1(\beta_2, 0, 0) > 0$ and $\pi_2(\beta_2, 0, 0) > 0$.
- iii)* For any fixed $\beta_2 > \epsilon$, if T is chosen sufficiently large, then $\pi_1(\beta_2, 0, T) > 0$ and $\pi_2(\beta_2, 0, T) < 0$.
- iv)* There exist choices for $\beta_2 > \epsilon$ and S large so that $\pi_1(\beta_2, S, 0) < 0$ and $\pi_2(\beta_2, S, 0) = 0$.

We consider the period map $\Pi(\beta_2, \beta_3, \beta_5) = (\pi_1(\beta_2, \beta_3, \beta_5), \pi_2(\beta_2, \beta_3, \beta_5))$. We choose β_2 , S , and T so that $\pi_1(\beta_2, 0, T) > 0$, $\pi_2(\beta_2, 0, T) < 0$, $\pi_1(\beta_2, S, 0) < 0$, and $\pi_2(\beta_2, S, 0) = 0$. Since β_2 is then a fixed value, we may consider $\pi_1 = \pi_1(\beta_3, \beta_5)$ and $\pi_2 = \pi_2(\beta_3, \beta_5)$ as functions of only the two variables β_3 and β_5 . Hence Π is a map from \mathbb{R}^2 to \mathbb{R}^2 . By the monotonic behavior of π_1 and π_2 on each τ_j , it follows that the image of $\tau_1 \cup \tau_2 \cup \tau_3 \cup \tau_4$ under Π is a homotopically nontrivial loop in $\mathbb{R}^2 \setminus \{(0, 0)\}$. Thus a zero for the period map Π lies in the region bounded by the curves τ_j . Hence the period problem associated to M_1^{+-} is solvable.

We prove items (i),(ii),(iii),(iv) above by studying the conjugate surface of the original one-eighth portion bounded by planar geodesics B_1, \dots, B_7 . The conjugate surface is a graph \mathcal{B} with respect to the x_2 direction over the rectangle $\{(x_1, 0, x_3) \in \mathbb{R}^3 \mid 0 \leq x_1 \leq \beta_2, 0 \leq x_3 \leq \epsilon\}$ in the x_1x_3 -plane, and its boundary, the conjugate contour, consists of seven lines B_1^*, \dots, B_7^* corresponding to the planar geodesics B_1, \dots, B_7 in the boundary of the original surface. Since conjugation preserves lengths, we have $\beta_j = \text{Length}(B_j) = \text{Length}(B_j^*)$. Thus B_1^* and B_7^* are each infinite rays with a single endpoint, and B_2^*, \dots, B_6^* are each finite line segments. The singular points of the conjugate contour are $V_j^* = B_j^* \cap B_{j+1}^*$ for $j = 1, \dots, 6$, corresponding to the points V_j on the original surface. B_1^* is the ray with endpoint $(\beta_2, -\beta_3, \epsilon)$ pointing in the direction of the positive x_2 -axis. B_2^* is the line segment with endpoints $(\beta_2, -\beta_3, \epsilon)$ and $(0, -\beta_3, \epsilon)$. B_3^* is the line segment with endpoints $(0, -\beta_3, \epsilon)$ and $(0, 0, \epsilon)$. B_4^* is the line segment with endpoints $(0, 0, \epsilon)$ and $(0, 0, 0)$. B_5^* is the line segment with endpoints $(0, 0, 0)$ and $(0, \beta_5, 0)$. B_6^* is the line segment with endpoints $(0, \beta_5, 0)$ and $(\beta_2, \beta_5, 0)$. B_7^* is the ray with endpoint $(\beta_2, \beta_5, 0)$ pointing in the direction of the positive x_2 -axis.

We denote this conjugate graph by $\mathcal{B}(\beta_2, \beta_3, \beta_5)$, since it depends on the values of β_2 , β_3 and β_5 . (It also depends on ϵ , but ϵ will remain fixed, so we do not notate this dependence.)

Proof of (i): Choose nonnegative values β_3 , $\tilde{\beta}_3$, and β_5 , with $\beta_3 < \tilde{\beta}_3$, and choose any $\beta_2 > \epsilon$. Then the interior of the graph $\mathcal{B}(\beta_2, \beta_3, \beta_5)$ lies above the interior of $\mathcal{B}(\beta_2, \tilde{\beta}_3, \beta_5)$ with respect to the x_2 direction, by Remark 3.1. These two graphs have the line B_4^* in common, and it follows that as one travels from V_3^* to V_4^* along B_4^* , the normal vector along B_4^* of $\mathcal{B}(\beta_2, \beta_3, \beta_5)$ is turning ahead of the normal vector along B_4^* of $\mathcal{B}(\beta_2, \tilde{\beta}_3, \beta_5)$. Furthermore, by the maximum principle these two normal vectors can never be equal in the interior of B_4^* . This means that on the original surfaces the normal vector along B_4 for $\beta_2, \beta_3, \beta_5$ is turning strictly ahead of the normal vector along B_4 for $\beta_2, \tilde{\beta}_3, \beta_5$, with respect to arc length. Since $\text{Length}(B_4) = \text{Length}(B_4^*) = \beta_4 = \epsilon$ is independent of β_3 , it follows that $\pi_1(\beta_2, \beta_3, \beta_5) > \pi_1(\beta_2, \tilde{\beta}_3, \beta_5)$.

We have just shown that for each fixed β_2 and β_5 , π_1 is a strictly decreasing function of β_3 . Similar arguments show the other parts of (i).

Proof of (ii): If $\beta_3 = \beta_5 = 0$, then V_2 coincides with V_3 and V_4 coincides with V_5 . The conjugate graph of this surface is unique, by Theorem 3.3, hence the surface is unique. Therefore it is M_1 . The embeddedness of M_1 implies that $\pi_2(\beta_2, 0, 0) > 0$.

The surface M_1 contains a vertical line, and this line divides both M_1 and B_4 into two congruent pieces. Let \hat{B}_4 be the half of B_4 that connects the midpoint of B_4 to $V_3 = V_2$. Let \hat{M}_1 be the congruent piece of M_1 bounded by B_1 , B_2 , \hat{B}_4 , and the vertical line. Since \hat{M}_1 has a single Scherk-type end whose normal is parallel to the x_1 axis, the maximum principle implies that the x_2 coordinate function on M_1 cannot be maximized in the interior of M_1 . Furthermore, as B_2 is a planar geodesic in a plane parallel to the x_2x_3 -plane, the boundary maximum principle implies that x_2 cannot be maximized on B_2 . Similarly, x_2 cannot be maximized on the interior of \hat{B}_4 . Therefore the value of the x_2 coordinate at $V_2 = V_3$ is strictly less than the value of the x_2 coordinate at the midpoint of B_4 . So $\pi_1(\beta_2, 0, 0) > 0$.

Proof of (iii): Fix $\beta_2 > \epsilon$, and choose $\beta_3 = 0$ and $\beta_5 = T \gg 1$. Then $\lim_{T \rightarrow \infty} \mathcal{B}(\beta_2, 0, T)$ is a graph bounded by B_1^* , B_2^* , B_4^* , and an infinite ray with endpoint at V_4^* pointing in the direction of the positive x_2 -axis. This graph has a single Scherk-type end of width $\sqrt{\beta_2^2 + \epsilon^2}$. (The fact that this limiting behavior occurs follows from the arguments in [JS]. In this proof we will consider various limit surfaces, and in all cases the existence of the limit graph follows from [JS].)

The original surface corresponding to $\lim_{T \rightarrow \infty} \mathcal{B}(\beta_2, 0, T)$ via conjugation is bounded by the planar geodesics B_1 , B_2 , B_4 , and an infinite version of B_5 . It has a single non-vertical Scherk-type end of width $\sqrt{\beta_2^2 + \epsilon^2}$. On $\lim_{T \rightarrow \infty} \mathcal{B}(\beta_2, 0, T)$, the maximum principle implies that its normal vector \vec{N} along B_4^* lies within a 90° geodesic arc of the unit sphere (so this is also true along B_4), and thus the x_2 coordinate at V_4 is greater than the x_2 coordinate at $V_2 = V_3$ on the original surface, so $\lim_{T \rightarrow \infty} \pi_1(\beta_2, 0, T) > 0$. Hence $\pi_1(\beta_2, 0, T) > 0$ for T sufficiently large.

Now we consider the limiting conjugate surface $\lim_{T \rightarrow \infty} (\mathcal{B}(\beta_2, 0, T) - (0, T, 0))$, which is a graph bounded by B_6^* , B_7^* , an infinite version of B_5^* equal to the negative x_2 axis, and a complete line through $(\beta_2, 0, \epsilon)$ parallel to the x_2 -axis. This conjugate surface has two ends of Scherk-type. One end has width ϵ and the other has width $\sqrt{\beta_2^2 + \epsilon^2}$. The original surface that corresponds to it via conjugation is bounded by B_6 , B_7 , an infinite version of B_5 , and a complete infinite version of B_1 . It has two ends, again of width ϵ and $\sqrt{\beta_2^2 + \epsilon^2} > \epsilon$. Because of the relative widths of the ends on this original surface, we see that the x_2 coordinate at V_5 is greater than the x_2 coordinate at V_6 , so $\lim_{T \rightarrow \infty} \pi_2(\beta_2, 0, T) < 0$. Hence $\pi_2(\beta_2, 0, T) < 0$ for T sufficiently large. (See Figure 11.)

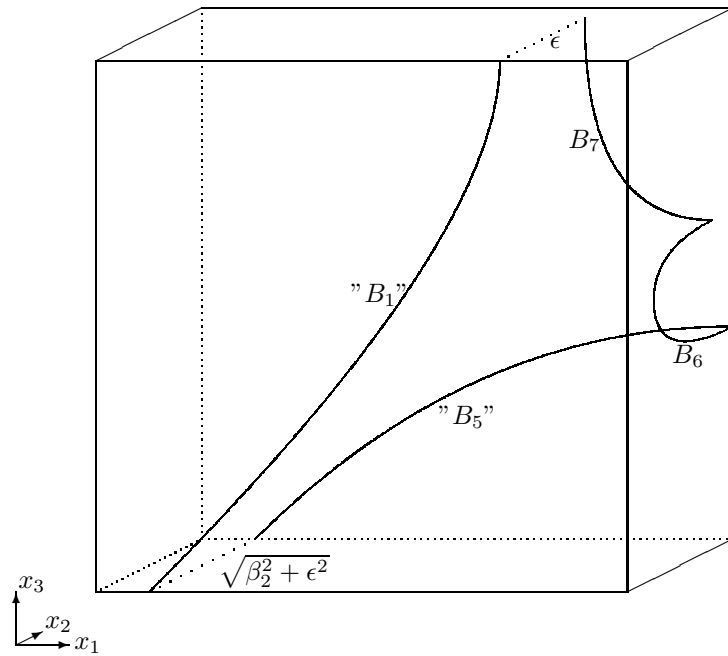


Figure 11: The original limit surface described at the end of the proof of (iii).

Proof of (iv): Choose $\beta_2 > \epsilon$, $\beta_5 = 0$, and $\beta_3 = S \gg 1$. We consider the limiting conjugate surface $\lim_{S \rightarrow \infty} \mathcal{B}(\beta_2, S, 0)$, which is a graph bounded by B_4^* , B_6^* , B_7^* , an infinite ray with endpoint at V_3^* pointing in the direction of the negative x_2 -axis, and a complete line through $(\beta_2, 0, \epsilon)$ parallel to the x_2 -axis. This conjugate surface has two ends of Scherk-type. One end has width ϵ and the other has width β_2 . The original surface that corresponds to it via conjugation is bounded by B_4 , B_6 , B_7 , an infinite ray version of B_3 , and a complete infinite version of B_1 . It has two ends, again one of width ϵ and the other of width β_2 .

We now consider what happens to the original surface corresponding to $\lim_{S \rightarrow \infty} \mathcal{B}(\beta_2, S, 0)$ as $\beta_2 \searrow \epsilon$ and as $\beta_2 \nearrow \infty$.

The conjugate surface $\lim_{\beta_2 \rightarrow \epsilon} (\lim_{S \rightarrow \infty} \mathcal{B}(\beta_2, S, 0))$ is a graph with respect to the x_2 direction over the square $\{(x_1, 0, x_3) \in \mathbb{R}^3 \mid 0 \leq x_1, x_3 \leq \epsilon\}$. It is bounded by the infinite ray B_7^* with endpoint $(\epsilon, 0, 0)$ pointing in the direction of the positive x_2 -axis, the line segment B_6^* from $(\epsilon, 0, 0)$ to $(0, 0, 0)$, the line segment B_4^* from $(0, 0, 0)$ to $(0, 0, \epsilon)$, and the infinite ray with endpoint $(0, 0, \epsilon)$ pointing in the direction of the negative x_2 -axis. The corresponding original surface is bounded by the planar geodesics B_4 , B_6 , B_7 , and a complete infinite version of B_1 . This original surface has two ends of Scherk-type, both of width ϵ .

Note that the graph $\lim_{\beta_2 \rightarrow \epsilon} (\lim_{S \rightarrow \infty} \mathcal{B}(\beta_2, S, 0))$ contains the line segment from $(0, 0, 0)$ to $(\epsilon, 0, \epsilon)$ and is symmetric with respect to rotation about this line, by uniqueness in Theorem 3.3 and by Theorem 3.1. The maximum principle then implies that the normal vector \vec{N} along each of B_4^* and B_6^* is contained in a 90° geodesic arc of the unit sphere, and thus the x_2 coordinate at V_3 is greater than the x_2 coordinate at $V_4 = V_5$ in the corresponding original surface, and the x_2 coordinate at V_3 equals the x_2 coordinate at V_6 . Therefore $\lim_{\beta_2 \rightarrow \epsilon} (\lim_{S \rightarrow \infty} \pi_2(\beta_2, S, 0)) = -\lim_{\beta_2 \rightarrow \epsilon} (\lim_{S \rightarrow \infty} \pi_1(\beta_2, S, 0)) > 0$. Hence for β_2 sufficiently close to ϵ and S sufficiently large, we have $\pi_2(\beta_2, S, 0) > 0$.

The limiting conjugate surface $\lim_{\beta_2 \rightarrow \infty} (\lim_{S \rightarrow \infty} \mathcal{B}(\beta_2, S, 0))$ is a portion of a helicoid (this follows from [JS]) bounded by the positive x_1 -axis, the line segment B_4^* from $(0, 0, 0)$ to $(0, 0, \epsilon)$, and an infinite ray with endpoint $(0, 0, \epsilon)$ pointing in the direction of the negative x_2 -axis. On the corresponding original surface, one eighth of a catenoid, we then have that B_4 is a quarter circle of radius $2\epsilon/\pi$. Thus $\lim_{\beta_2 \rightarrow \infty} (\lim_{S \rightarrow \infty} \pi_1(\beta_2, S, 0)) = -2\epsilon/\pi$. Since the original surface corresponding to $\lim_{S \rightarrow \infty} \mathcal{B}(\beta_2, S, 0)$ has two Scherk-type ends of width ϵ and β_2 , it follows that $\lim_{\beta_2 \rightarrow \infty} (\lim_{S \rightarrow \infty} (\pi_1(\beta_2, S, 0) + \pi_2(\beta_2, S, 0))) = \lim_{\beta_2 \rightarrow \infty} (\epsilon - \beta_2) = -\infty$. Thus for β_2 and S sufficiently large, we have $\pi_2(\beta_2, S, 0) < 0$.

Therefore for some large S and some value of $\beta_2 > \epsilon$, we have $\pi_2(\beta_2, S, 0) = 0$. If, for this S and β_2 , we have $\pi_1(\beta_2, S, 0) \geq 0$, then the original surface corresponding to this β_2 , $\beta_3 = S$, and $\beta_5 = 0$ would contain some point in $B_4 \cup B_6$ where x_2 has a local maximum and where the tangent plane is parallel to the x_1x_3 -plane. This contradicts the maximum principle. So, for this S and β_2 , we have $\pi_1(\beta_2, S, 0) < 0$. This shows **(iv)**.

This completes the proof of the solvability of the period problem associated to M_1^{+-} . Note that $\Pi(\tau_1 \cup \tau_2 \cup \tau_3 \cup \tau_4)$ changes continuously under continuous changes of β_2 , so for all β_2 sufficiently close to the β_2 chosen above, $\Pi(\tau_1 \cup \tau_2 \cup \tau_3 \cup \tau_4)$ is still a homotopically nontrivial loop in $\mathbb{R}^2 \setminus \{(0, 0)\}$, and so the period problem remains solvable. Hence β_2 in a small open interval serves as a deformation parameter for the surface, thereby yielding a one-parameter family of these surfaces. Since each eighth of the surface is embedded, and the maximum principle tells us this embedded surface lies in the bounding box determined by the planar curves B_j , each surface in the family is embedded. This completes the proof.

The proof of Theorem 9.1 cannot be directly adapted to prove existence of M_k^{+-} for $k \geq 2$. However,

numerical evidence suggests that the M_k^{+-} exist for $k \geq 2$ as well, so we make this conjecture (see Figure 3).

Conjecture 9.1 *There exists a one-parameter family of genus three, embedded minimal surfaces M_k^{+-} with $4k$ Scherk-type ends, for all $k \geq 2$.*

In fact, numerical evidence also suggests that there exists a wide variety of minimal surfaces with Scherk-type ends and more handles of both $+$ and $-$ type. (See Figure 12.)

10 Appendix: a proof of Lemma 4.1

The first part of Lemma 4.1 is intended only to be an intuitive aid, saying that "each collection of surfaces results from adding ends and handles to M_1 ". However, a rigorous proof is required for the statement that "the period problems arising from the additional ends are all solved by requiring $\epsilon = \text{length}(A_i) = \text{length}(B_j)$ ".

For each surface, we always begin by choosing one-eighth of the original fundamental piece of the surface. This one-eighth piece is bounded by planar geodesics, and its conjugate surface is bounded by portions of lines. Before we consider any period problems, we must first establish existence of this conjugate surface, which then implies the existence of the original one-eighth piece (without solving for period problems yet).

The conjugate pieces exist because they are Jenkins-Serrin graphs. In all the cases we consider, they are Jenkins-Serrin graphs over a rectangle, and the boundary data is a finite constant over each of three sides of the boundary of the rectangle. On the fourth side, the boundary data alternates between $+\infty$ and $-\infty$ along adjacent intervals. The jump discontinuities occur only at the corners of the rectangle and at points along the fourth side where the boundary data changes from $+\infty$ to $-\infty$.

Recall Theorem 3.3. In our case, by applying a rigid motion and a homothety of \mathbb{R}^3 , we may assume without loss of generality that $D = \{(x_1, x_2) \in \mathbb{R}^2 \mid 0 \leq x_1 \leq \delta, 0 \leq x_2 \leq 1\}$ for some positive δ , that there are three C_k 's which we define as $C_1 = D \cap \{(x_1, 0) \in \mathbb{R}^2\}$, $C_2 = D \cap \{(\delta, x_2) \in \mathbb{R}^2\}$, and $C_3 = D \cap \{(x_1, 1) \in \mathbb{R}^2\}$, and that there are ℓ number of A_i 's and B_j 's, all of length $\frac{1}{\ell}$ alternating along $D \cap \{(0, x_2) \in \mathbb{R}^2\}$. Notice here that we have already incorporated the condition of Lemma 4.1, that is, that

$$\epsilon = \text{length}(A_i) = \text{length}(B_j) = \frac{1}{\ell}.$$

Existence and uniqueness of a solution u to the minimal surface equation with the given boundary data now follows from Theorem 3.3. (The conditions on the polygons \mathcal{P} are trivially satisfied, since no such \mathcal{P} exists for the boundary conditions we are using.) Furthermore, the results in [JS] imply that u is finite at every point in the interior of D .

Let M denote the smallest closed minimal surface that contains the graph u . (Here we use the word "closed" in the sense that M contains all of its accumulation points.) Hence the interior of M is the interior of the graph u , and M contains its boundary ∂M , and the image of the vertical projection of M to the x_1x_2 -plane is $D \setminus \{(0, x_2) \in \mathbb{R}^2 \mid x_2 \neq \frac{k}{\ell} \text{ some } k \in \mathbb{Z}\}$.

We now prove Lemma 4.1 in a series of eight claims.

Claim 1: M has finite total absolute curvature.

Proof. Following the proof in [JS], p 334, u is the limit of a subsequence of minimal graphs $\{u_n\}_{n=1}^{\infty}$ over $\text{Int}(D)$. The minimal graphs u_n are determined by replacing the boundary condition $+\infty$ by $+n$ on each A_i ,

replacing the boundary condition $-\infty$ by $-n$ on each B_j , and leaving the boundary data on $C_1 \cup C_2 \cup C_3$ unchanged.

First we show that the total absolute curvature of the graph of u_n is bounded above by a finite bound independent of n , which follows easily from the Gauss-Bonnet formula. The boundary of u_n is polygonal with at most $2\ell + 6$ boundary line segments, and at each intersection of adjacent boundary line segments the angle of intersection is $\frac{\pi}{2}$. Hence the total geodesic curvature of the boundary curve for the graph u_n is at most $\frac{\pi}{2}(2\ell + 6)$. The Gauss-Bonnet formula then implies

$$\int_{\text{Graph}(u_n)} |K| dA \leq \pi(\ell + 1) \quad \forall n, \quad (10.1)$$

where dA is the area form on $\text{Graph}(u_n)$ induced by \mathbb{R}^3 , and K is the intrinsic Gaussian curvature of $\text{Graph}(u_n)$.

Now we claim that for any compact convex domain $D' \subset \text{Int}(D)$, there exists a subsequence $\{n_j\}_{j=1}^{\infty}$ such that the total absolute curvature of the graphs of u_{n_j} restricted to the domain D' converges to the total absolute curvature of the graph of u restricted to D' . That is, we claim that

$$\int_{\text{Graph}(u_{n_j}|_{D'})} |K| dA \rightarrow \int_{\text{Graph}(u|_{D'})} |K| dA \quad (10.2)$$

as $n_j \rightarrow \infty$. This follows from the fact that, as shown in [JS], $u_n|_{D'}$ converges uniformly to $u|_{D'}$ as $n \rightarrow \infty$. The convergence (10.2) is essentially known, and arguments showing it exist in several places. For example, a proof is contained in the arguments proving Theorem 2 in [MY]. The arguments in [MY] are intended for more general ambient spaces, and when the ambient space is \mathbb{R}^3 the arguments in [MY] can be considerably simplified. A simpler argument for the \mathbb{R}^3 case can be found in section III.2 of [C].

For completeness, in this paragraph we outline an argument showing (10.2). We know that the u_n converge uniformly to u over D' , by [JS]. These graphs $u_n|_{D'}$ (resp. $u|_{D'}$) are graphs over convex domains in the x_1x_2 -plane and hence are the unique compact minimal surfaces with respect to their boundaries. Hence they coincide as surfaces in \mathbb{R}^3 with the Douglas-Rado solutions $f_n : B^2 := \{(u, v) \in \mathbb{R}^2 \mid u^2 + v^2 \leq 1\} \rightarrow \mathbb{R}^3$ (resp. $f : B^2 \rightarrow \mathbb{R}^3$) for their boundaries. That is, the surfaces $f_n(B^2)$ and $\{(x_1, x_2, u_n(x_1, x_2)) \in \mathbb{R}^3 \mid (x_1, x_2) \in D'\}$ (resp. $f(B^2)$ and $\{(x_1, x_2, u(x_1, x_2)) \in \mathbb{R}^3 \mid (x_1, x_2) \in D'\}$) coincide. The parametrizations f_n and f have the advantage that they are conformal, hence the coordinate functions $f_n^i, f^i, i = 1, 2, 3$ are harmonic on B^2 . Using arguments similar to those we use later to prove Claim 6 of this note, we can see that in fact

$$\frac{\partial u_n}{\partial x_1} \rightarrow \frac{\partial u}{\partial x_1}, \quad \frac{\partial u_n}{\partial x_2} \rightarrow \frac{\partial u}{\partial x_2}$$

converge uniformly over D' as well. (This is equivalent to showing that the normal vectors of the graphs converge uniformly over D' .) Once we know that first derivatives of u_n also converge uniformly, the arguments in the proof of Lemma 3.2 and the remark following it in [C] can be applied: using the three-point condition as in [C], we can find a subsequence f_{n_j} of the f_n which converge uniformly to f on ∂B^2 . Since the functions $f_{n_j}^i, f^i$ are harmonic, and hence the functions $|f_{n_j}^i - f^i|$ always attain their maximums on ∂B^2 , we conclude that $f_{n_j} \rightarrow f$ uniformly on all of B^2 . Uniform convergence for harmonic functions implies that the convergence is smooth (this is a basic property of harmonic functions, see, for example, Theorem 2.10 of [GT]). We conclude that the Douglas-Rado solutions f_{n_j} converge smoothly to f . Hence the total absolute curvature of the graphs $u_{n_j}|_{D'}$ converges to the total absolute curvature of the graph $u|_{D'}$. This shows the convergence (10.2).

If the total absolute curvature of M is strictly greater than $\pi(\ell + 1)$, then there exists some compact convex domain $D' \subset \text{Int}(D)$ such that the graph of $u|_{D'}$ has total absolute curvature strictly greater than $\pi(\ell + 1)$. However, then the convergence (10.2) contradicts equation (10.1). Therefore the total absolute curvature of M is at most $\pi(\ell + 1)$, and Claim 1 is shown.

Claim 2: There are only a finite number of points of M at which the tangent plane is horizontal.

Proof. The proof below is simply a modification of an argument in the proof of Theorem 3.1 of [MW].

Consider the Gauss map $G : M \rightarrow S^2 = \{(x_1, x_2, x_3) \in \mathbb{R}^3 \mid x_1^2 + x_2^2 + x_3^2 = 1\}$. M is the closure of the graph u , so M is orientable, and so G is well-defined. We can define G so that $G(M) \subset S^2 \cap \{(x_1, x_2, x_3) \in \mathbb{R}^3 \mid x_3 \geq 0\}$. With respect to conformal coordinates on M , G is a holomorphic map from M to the upper hemisphere of S^2 , hence G is a branched covering with boundary into the upper hemisphere. Furthermore, since ∂M consists of portions of lines parallel to the coordinate axes in \mathbb{R}^3 ,

$$G(\partial M) \subset \{(x_1, x_2, x_3) \in S^2 \mid x_1 = 0 \text{ or } x_2 = 0 \text{ or } x_3 = 0\} \cap \{(x_1, x_2, x_3) \in \mathbb{R}^3 \mid x_3 \geq 0\}.$$

Therefore the covering degree of G is a constant on each of the four sets

$$\begin{aligned} &\{(x_1, x_2, x_3) \in S^2 \mid x_1 > 0, x_2 > 0, x_3 > 0\}, & \{(x_1, x_2, x_3) \in S^2 \mid x_1 < 0, x_2 > 0, x_3 > 0\}, \\ &\{(x_1, x_2, x_3) \in S^2 \mid x_1 > 0, x_2 < 0, x_3 > 0\}, & \{(x_1, x_2, x_3) \in S^2 \mid x_1 < 0, x_2 < 0, x_3 > 0\}. \end{aligned}$$

By Claim 1, these four constant covering degrees are all finite. If the inverse image $G^{-1}(\vec{e}_3 = (0, 0, 1))$ were to contain infinitely many points of M , then at least one of these four constant covering degrees would not be finite. Hence $G^{-1}(\vec{e}_3 = (0, 0, 1))$ is a finite set, showing Claim 2.

Let $P_s = \{(x_1, x_2, s) \in \mathbb{R}^3\}$ be the horizontal plane in \mathbb{R}^3 of height s . An immediate corollary to Claim 2 is the following Claim 3. In Claim 3, by "nonsingular curves of \mathbb{R}^3 ", we mean curves of \mathbb{R}^3 which are 1-dimensional submanifolds with boundary.

Claim 3: There exists a constant $L > 0$ such that, for all $L' > L$, $P_s \cap M, s \in [L, L']$ (resp. $s \in [-L', -L]$) is a smooth deformation (with respect to s) from $P_L \cap M$ to $P_{L'} \cap M$ (resp. from $P_{-L} \cap M$ to $P_{-L'} \cap M$) through an embedded collection of nonsingular curves of \mathbb{R}^3 .

Proof. A singularity in this deformation can only occur at a point of M where the tangent plane is horizontal. By Claim 2, we can choose L large enough that no such horizontal points exist in $\{(x_1, x_2, x_3) \in M \mid x_3 \geq L\}$ nor in $\{(x_1, x_2, x_3) \in M \mid x_3 \leq -L\}$. This proves Claim 3.

Thus, by Claim 3, for any $L' > L$, $M \cap \{(x_1, x_2, x_3) \in \mathbb{R}^3 \mid x_3 \in [L, L']\}$ consists of a finite number of components, and each component is an embedded disk bounded by two vertical line segments, and one curve in $P_{L'}$, and one curve in P_L . We choose any component M_{comp} of $M \cap \{(x_1, x_2, x_3) \in \mathbb{R}^3 \mid x_3 \in [L, L']\}$ and extend it by rotations of π radians about vertical boundary lines (this can be done, and the extended surfaces are smooth, by the Schwarz reflection principle, Theorem 3.1). Extending M_{comp} (and its extended surfaces) by these rotations a finite number of times results in a larger compact surface which still has only two vertical boundary line segments, and one boundary curve in $P_{L'}$, and one boundary curve in P_L . We make these rotational extensions enough times so that the distance in \mathbb{R}^3 from any point in M_{comp} to the

two boundary vertical line segments of the extended surface is greater than $\frac{1}{4}(L' - L)$. We call this extended surface M_{comp}^{ext} – it is an immersed compact disk in \mathbb{R}^3 , and is not necessarily embedded. (We will later see that M_{comp}^{ext} is indeed embedded for L large enough.)

Claim 4: M_{comp}^{ext} is strongly stable.

Proof. The image $G(M_{comp})$ is contained in the upper hemisphere of S^2 and does not contain the north pole \vec{e}_3 . Since M_{comp}^{ext} is comprised of a finite number of pieces congruent to M_{comp} which are all images of vertical rotations of M_{comp} , it follows that $G(M_{comp}^{ext})$ is also contained in the upper hemisphere and does not contain \vec{e}_3 . In particular, the area of $G(M_{comp}^{ext})$ in S^2 is strictly less than 2π .

Theorem 1.2 of [BdC] tells us that if the area of $G(M_{comp}^{ext})$ is less than 2π , then M_{comp}^{ext} is stable. The map G is not required to be an injection in order for this theorem to hold, and the minimal surface need only be an immersion – it does not need to be an embedding. Furthermore, in [BdC] the word *stable* is used in the strong sense; that is, a minimal surface is stable if the second derivative of area for any smooth nontrivial boundary-preserving variation is *strictly* positive. This shows Claim 4.

For an oriented minimal surface $\mathcal{M} \subset \mathbb{R}^3$, let $\text{dist}_{\mathcal{M}}(A, B)$ be the intrinsic distance in \mathcal{M} between two sets $A, B \subset \mathcal{M}$. For each point $q \in \mathcal{M}$, let K_q be the Gaussian curvature of \mathcal{M} at q , and let \vec{N}_q be the oriented unit normal vector of \mathcal{M} at q . Let $\vec{e}_1 = (1, 0, 0)$, and let $\langle \cdot, \cdot \rangle$ be the standard inner product on \mathbb{R}^3 . Let $\text{dist}_{\mathbb{R}^3}(A, B)$ be the distance in \mathbb{R}^3 between two sets $A, B \subset \mathbb{R}^3$.

By Corollary 4 of [S] there exists a universal constant c such that

$$|K_q| < \frac{c}{(\text{dist}_{\mathcal{M}}(q, \partial\mathcal{M}))^2},$$

where \mathcal{M} is any compact stable minimal surface in \mathbb{R}^3 , and q is any point in \mathcal{M} . This result (just like Theorem 1.2 of [BdC]) does not require the surface \mathcal{M} to be embedded – only immersed. The constant c is universal in the sense that it is independent of the choice of \mathcal{M} . (See Theorem 16.20 of [GT] and Theorem 11.1 of [O] for related results.)

Claim 5: On the surface $\hat{M} := M_{comp} \cap \{(x_1, x_2, x_3) \in \mathbb{R}^3 \mid x_3 \in [\frac{1}{4}L' + \frac{3}{4}L, \frac{3}{4}L' + \frac{1}{4}L]\}$, the Gaussian curvature K is uniformly bounded by

$$|K| < \frac{16c}{(L' - L)^2}.$$

Proof. M_{comp}^{ext} is a compact minimal surface in \mathbb{R}^3 , which is strongly stable by Claim 4. For all $q \in \hat{M}$, $\text{dist}_{M_{comp}^{ext}}(q, \partial M_{comp}^{ext}) \geq \frac{L' - L}{4}$. Now we apply Corollary 4 of [S] and Claim 5 is proven.

Assume that L' is chosen large enough that $\frac{8\sqrt{c\delta}}{L' - L} < 1$.

Claim 6: At every point of $M_{comp} \cap \{(x_1, x_2, x_3) \in \mathbb{R}^3 \mid x_3 \in [\frac{3}{8}L' + \frac{5}{8}L, \frac{5}{8}L' + \frac{3}{8}L]\}$, we have

$$|\langle \vec{N}, \vec{e}_1 \rangle| \geq \sqrt{1 - \frac{8\sqrt{c\delta}}{L' - L}}.$$

Proof. Suppose some point $p \in M_{comp} \cap \{(x_1, x_2, x_3) \in \mathbb{R}^3 \mid x_3 \in [\frac{3}{8}L' + \frac{5}{8}L, \frac{5}{8}L' + \frac{3}{8}L]\}$ has normal \vec{N}_p so that $|\langle \vec{N}_p, \vec{e}_1 \rangle| < \sqrt{1 - \frac{8\sqrt{c\delta}}{L' - L}}$. Then there is a tangent vector \vec{T} at p such that $\langle \vec{T}, \vec{e}_1 \rangle > \sqrt{\frac{8\sqrt{c\delta}}{L' - L}}$. Assume

L' and c are chosen large enough that $L' - L > 1$ and $c > 1024 \cdot \delta^2$. Consider a unit-speed geodesic $\gamma(t) \subset \hat{M}$, $t \in [0, (L' - L)/8]$ so that $\gamma(0) = p$ and $\gamma'(0) = \vec{T}$, where $\iota = \frac{\partial}{\partial t}$. We define

$$t_0 := \sqrt{\frac{\delta(L' - L)}{2\sqrt{c}}}.$$

Since $L' > L + 1$ and $c > 1024 \cdot \delta^2$, we have that $t_0 < (L' - L)/8$ and hence $\gamma(t_0) \in \hat{M}$. Let $k_g(t)$ be the geodesic curvature of $\gamma(t)$. Since $|K_q| < \frac{16c}{(L' - L)^2}$ for all $q \in \hat{M}$ by Claim 5, and since \hat{M} is minimal, $|k_g(t)| < \frac{4\sqrt{c}}{(L' - L)}$ for all $t \in [0, (L' - L)/8]$. Thus $|\gamma''(t)| < \frac{4\sqrt{c}}{(L' - L)}$. Writing $\gamma(t) = (\gamma_1(t), \gamma_2(t), \gamma_3(t))$ in terms of coordinates in \mathbb{R}^3 , we have $|\gamma_1''(t)| < \frac{4\sqrt{c}}{(L' - L)}$. Then for $t \in [0, (L' - L)/8]$,

$$|\gamma_1'(t) - \gamma_1'(0)| = \left| \int_0^t \gamma_1''(s) ds \right| \leq \int_0^t |\gamma_1''(s)| ds < \frac{4\sqrt{c}}{L' - L} \cdot t,$$

and thus $\gamma_1'(t) > \gamma_1'(0) - \frac{4\sqrt{c}}{L' - L} \cdot t$. Therefore

$$\begin{aligned} \gamma_1(t_0) &\geq \gamma_1(t_0) - \gamma_1(0) = \int_0^{t_0} \gamma_1'(t) dt > \int_0^{t_0} \left(\gamma_1'(0) - \frac{4\sqrt{c}}{L' - L} t \right) dt = \\ &= \gamma_1'(0)t_0 - \frac{2\sqrt{c}}{L' - L} t_0^2 > \sqrt{\frac{8\sqrt{c}\delta}{L' - L}} \cdot t_0 - \frac{2\sqrt{c}}{L' - L} t_0^2 = \delta. \end{aligned}$$

The final inequality above follows from $\gamma_1'(0) = \langle \vec{T}, \vec{e}_1 \rangle > \sqrt{\frac{8\sqrt{c}\delta}{L' - L}}$, and the final equality follows from the definition of t_0 . This is a contradiction, since the vertical projection to the x_1x_2 -plane of the geodesic $\gamma(t) \subset \hat{M} \subset M$ is contained in D . This proves Claim 6.

Note that M_{comp} is one component of $M \cap \{(x_1, x_2, x_3) \in \mathbb{R}^3 \mid x_3 \in [L, L']\}$ and thus $M_{comp} = M_{comp}(L')$ depends on L' . We now wish to increase M_{comp} to a connected noncompact surface \tilde{M} that is independent of L' . Define

$$\tilde{M} := \cup_{L' > L} M_{comp}(L').$$

Thus $M_{comp}(L') \subset \tilde{M}$ for all L' , and \tilde{M} is a disk bounded by one curve in P_L and by two upward-pointing vertical rays r_1, r_2 with endpoints in P_L . Since $L' > L + \max(1, 8\sqrt{c}\delta)$ was arbitrary in the proof of Claim 6, an easy corollary of Claim 6 is the following:

Claim 7: The normal vector \vec{N} on \tilde{M} converges to $\pm \vec{e}_1$ at the end of \tilde{M} . More precisely, for all $\rho \in (0, 1)$, there exists $\mathcal{L}(\rho) > 0$ such that at all points $q \in \{(x_1, x_2, x_3) \in \tilde{M} \mid x_3 > \mathcal{L}(\rho)\}$, the normal \vec{N}_q satisfies $\|\vec{N}_q - \vec{e}_1\| < \rho$ or $\|\vec{N}_q + \vec{e}_1\| < \rho$.

Proof. We choose s so that $L' = 2s$. By Claim 6, if $L' > L + \max(1, 8\sqrt{c}\delta)$, then

$$\langle \vec{N}_q, \vec{e}_1 \rangle^2 \geq 1 - \frac{8\sqrt{c}\delta}{2s - L}$$

for every point $q \in P_s \cap M_{comp}$. Define

$$\vec{N}_q^\perp := \vec{N}_q - \langle \vec{N}_q, \vec{e}_1 \rangle \vec{e}_1,$$

Then $\|\vec{N}_q^\perp\|^2 \leq \frac{8\sqrt{c}\delta}{2s - L}$ and $\vec{N}_q \pm \vec{e}_1 = (\langle \vec{N}_q, \vec{e}_1 \rangle \pm 1)\vec{e}_1 + \vec{N}_q^\perp$. By a straightforward computation, choosing

$$s > \frac{16\sqrt{c}\delta + 3L}{3\rho^2} + 1$$

is sufficient to ensure

$$\min\|\vec{N}_q \pm \vec{e}_1\| < \rho \text{ and } L' > L + \max(1, 8\sqrt{c\delta}) .$$

Claim 7 is shown.

Using Claim 7 and elementary properties of conjugation, we now prove Lemma 4.1.

Note that $\text{dist}_{\mathbb{R}^3}(r_1, r_2) = \frac{k}{\ell}$ for some positive integer k . By Claim 7 and the original construction of the boundary data (i.e. the choices we made for the A_i, B_j) in the Jenkins-Serrin graph, we see that $k = 1$. Furthermore, by Claim 7, we have

$$\text{dist}_{\tilde{M}}(r_1, r_2) = \text{dist}_{\mathbb{R}^3}(r_1, r_2) = \frac{1}{\ell} . \quad (10.3)$$

Let \tilde{M}_{conj} be the conjugate surface of \tilde{M} . We have the following properties:

1. Since conjugation is an isometry, \tilde{M}_{conj} is bounded by one smooth curve of finite length, and two smooth curves \hat{r}_1, \hat{r}_2 of infinite length.
2. Since conjugation maps straight lines to planar geodesics, \hat{r}_1, \hat{r}_2 are two boundary planar geodesics of \tilde{M}_{conj} that are the images of the boundary rays r_1, r_2 , respectively, under conjugation.
3. Since conjugation preserves the Gauss map and hence also \vec{N} , \hat{r}_1 and \hat{r}_2 each lie in a horizontal plane. We call these two horizontal planes \hat{P}_1 and \hat{P}_2 , respectively.
4. Since the normal vector \vec{N} is preserved under conjugation, \vec{N} on \tilde{M}_{conj} converges to $\pm\vec{e}_1$ at the end of \tilde{M}_{conj} .
5. By property 4 above, $\text{dist}_{\mathbb{R}^3}(\hat{P}_1, \hat{P}_2) = \text{dist}_{\tilde{M}_{conj}}(\hat{r}_1, \hat{r}_2)$.
6. Since conjugation is an isometry, $\text{dist}_{\tilde{M}_{conj}}(\hat{r}_1, \hat{r}_2) = \text{dist}_{\tilde{M}}(r_1, r_2)$.

Finally, from equation (10.3) and properties 5 and 6 above, we conclude:

Claim 8: $\text{dist}_{\mathbb{R}^3}(\hat{P}_1, \hat{P}_2) = \frac{1}{\ell}$.

On the conjugate \tilde{M}_{conj} of $\tilde{M} \subset \{(x_1, x_2, x_3) \in M \mid x_3 \geq L\}$, the period problem at the end is a vertical translation comprised of one reflection through \hat{P}_1 composed with one reflection through \hat{P}_2 . Thus the period problem is a vertical translation of length exactly $\frac{2}{\ell}$, by Claim 8. Likewise, the same holds for the conjugate surface of any other components of $\{(x_1, x_2, x_3) \in M \mid x_3 \geq L\}$ and any components of $\{(x_1, x_2, x_3) \in M \mid x_3 \leq -L\}$ as well, when L is chosen large enough. Since the boundary behavior alternates between $+\infty$ and $-\infty$ along the alternating A_i 's and B_j 's, the normal vector of the graph u must alternately approach $+\vec{e}_1$ and $-\vec{e}_1$ along the A_i 's and B_j 's. Therefore, as one travels along the line segment $D \cap \{(0, x_2) \in \mathbb{R}^2\}$, the vertical direction of the translation periods at the ends of the conjugate surface of M alternates between upward and downward translations of length $\frac{2}{\ell}$.

Thus Lemma 4.1 is shown.

References

- [BdC] L. Barbosa, M. do Carmo. On the size of a stable minimal surface in \mathbb{R}^3 , *Amer. J. of Math.*, vol 98, no. 2, pg515-528, 1976.
- [C] R. Courant. Dirichlet's principle, conformal mapping, and minimal surfaces. Interscience Publishers, 1950.
- [DHKW] U. Dierkes, S. Hildebrandt, A. Küster, and O. Wohlrab. *Minimal Surfaces I*. Springer-Verlag, 1993.
- [GT] D. Gilbarg, N. S. Trudinger. Elliptic partial differential equations of second order. A series of comprehensive studies in mathematics 224, 2nd ed, Springer, revised third printing 1998.
- [JS] H. Jenkins, J. Serrin. Variational problems of minimal surface type II. Boundary value problems the minimal surface equation. *Arch. Rational Mech. Anal.*, 21:321-342, 1965.
- [K1] H. Karcher. Embedded minimal surfaces derived from Scherk's examples. *Manuscripta Math.*, 62:83-114, 1988.
- [K2] H. Karcher. *Construction of minimal surfaces*. Surveys in Geometry, 1-96, 1989. University of Tokyo, 1989, and Lecture Notes No. 12, SFB256, Bonn, 1989.
- [K3] H. Karcher. *Construction of higher genus embedded minimal surfaces*. Geometry and Topology of Submanifolds III, World Scientific, 1990, 174-191.
- [KP] H. Karcher, K. Polthier. Personal communications.
- [MR] W. H. Meeks, H. Rosenberg. The maximum principle at infinity for minimal surfaces in flat three-manifolds. *Commentari Mathematici Helvetici*, 65:255-270, 1990.
- [MY] W. H. Meeks, S. T. Yau. The classical Plateau problem and the topology of three-dimensional manifolds, *Topology* 21(4), 409-442, 1982.
- [MW] W. H. Meeks, B. White. Minimal surfaces bounded by convex curves in parallel planes, *Comm. Math. Helv.*, 66, p263-278, 1991.
- [O] R. Osserman. A survey of minimal surfaces. Dover Publications, 1986.
- [S] R. Schoen. Estimates for stable minimal surfaces in three dimensional manifolds, *Annals of Math. Stud.* 103, Princeton University Press, 1983.
- [T] E. Thayer. *Complete Minimal Surfaces in Euclidean Three Space*. PhD thesis, University of Massachusetts, Amherst, September 1994.
- [We] F. Wei. Some existence and uniqueness theorems for doubly periodic minimal surfaces. *Invent. Math.*, 109:113-136, 1992.
- [Wo] M. Wohlgemuth. Minimal surfaces of high genus with finite total curvature. *Arch. Ration. Mech. Anal.*, 137(1):1-25, 1997.

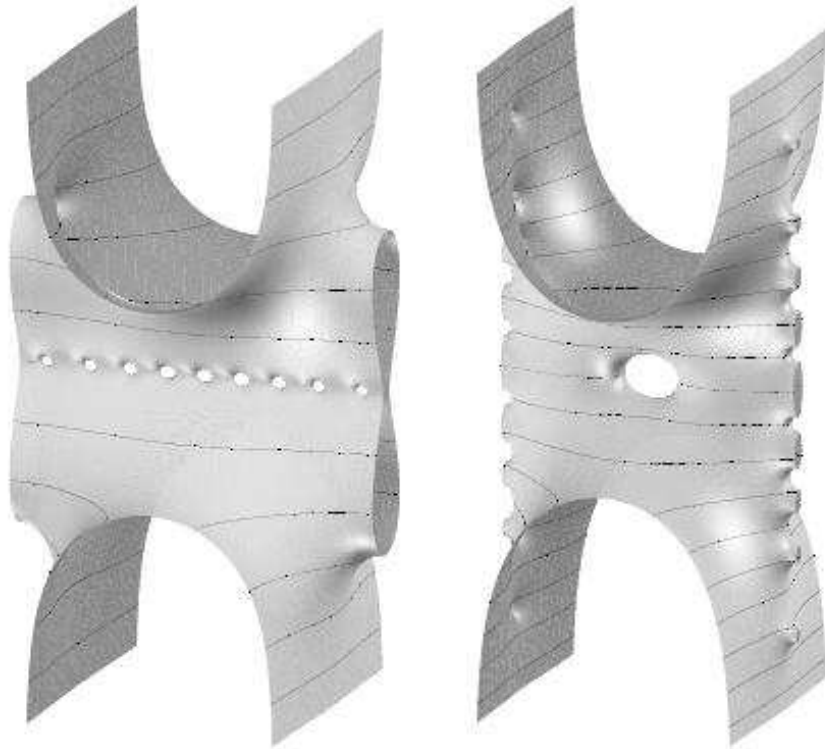


Figure 12: Fundamental pieces of M_1^{9+} (left) and $M_1^{+,8-}$ (right).

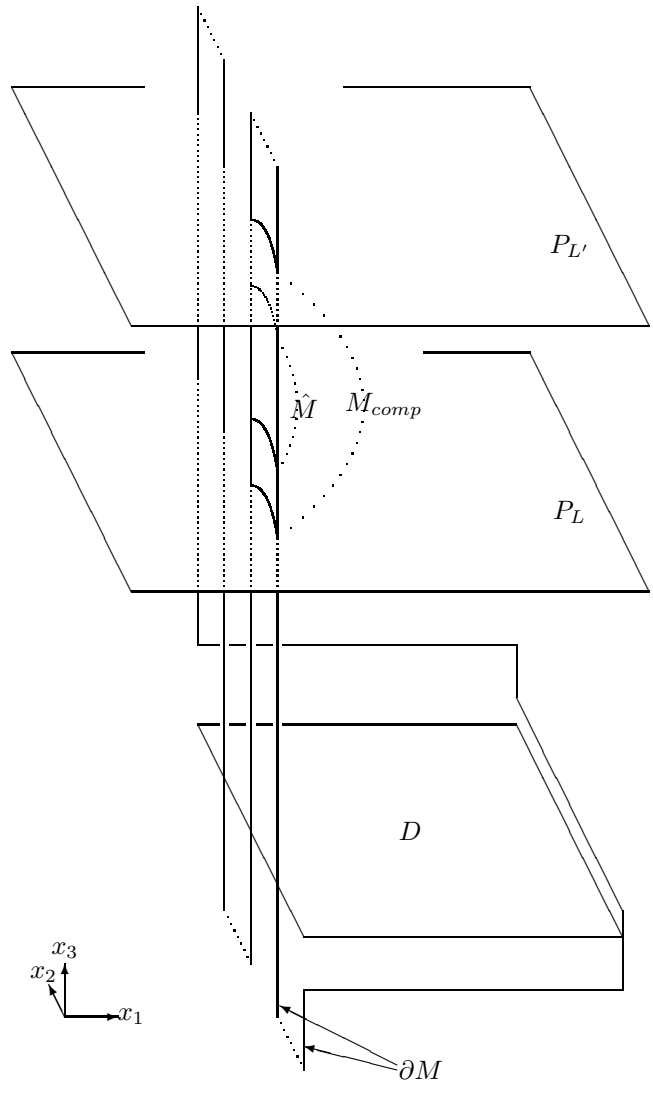


Figure 13: The location of \hat{M} , as defined in Claim 5.

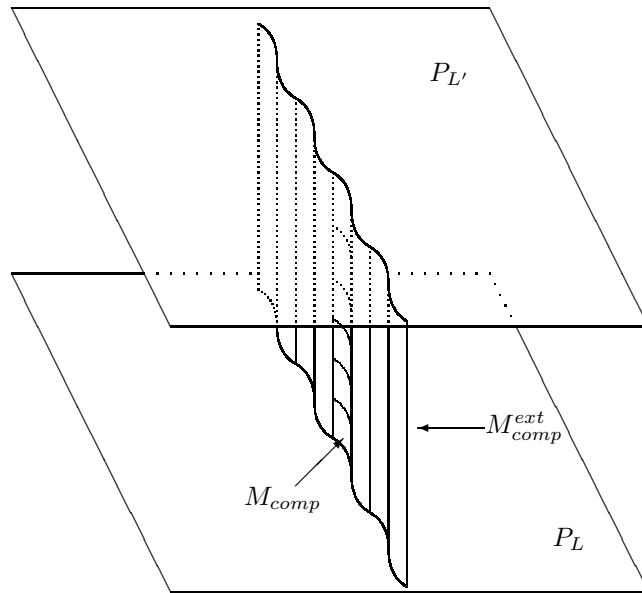


Figure 14: The construction of M_{comp}^{ext} .

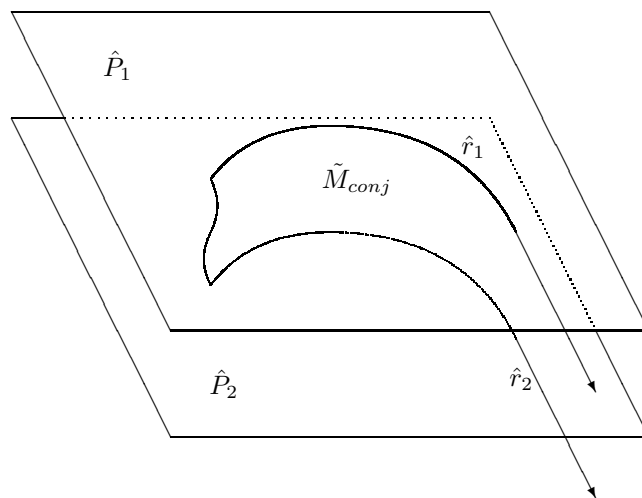


Figure 15: The conjugate surface of \tilde{M} .

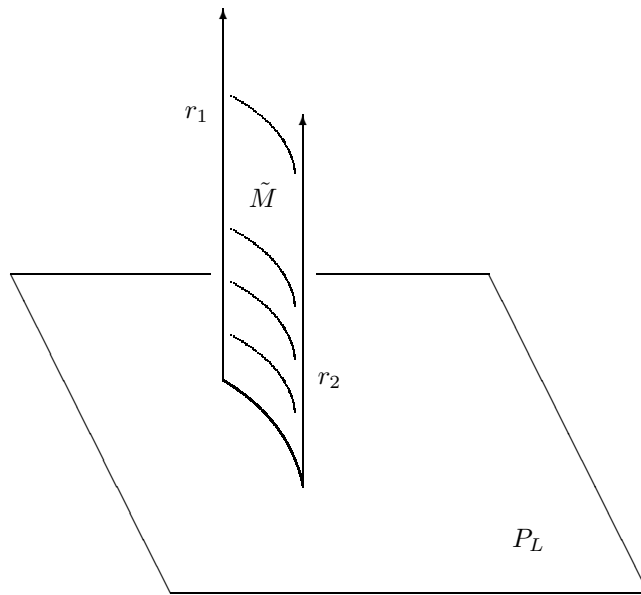


Figure 16: The surface \tilde{M} .